Contract DA 19-129-QM-1383
O.I. No. 9118

IMPACT DETERMINATIONS
FINAL REPORT

by
E. A. Ripperger

October 1962

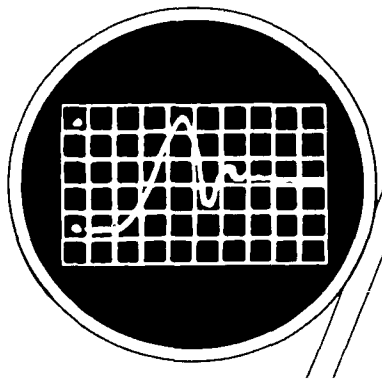

STRUCTURAL MECHANICS RESEARCH LABORATORY
THE UNIVERSITY OF TEXAS
BALCONES RESEARCH CENTER
AUSTIN, TEXAS

Contract DA 19-129-QM-1383

O.I. No. 9118

IMPACT DETERMINATIONS

FINAL REPORT

by

E. A. Ripperger

Prepared for

QUARTERMASTER
RESEARCH AND ENGINEERING
COMMAND

THE UNIVERSITY OF TEXAS

STRUCTURAL MECHANICS RESEARCH LABORATORY

Austin, Texas

October 26, 1962

The Structural Mechanics Research Laboratory

is cooperatively operated by

The Engineering Mechanics and Civil Engineering Departments

at

The Balcones Research Center

University of Texas

Austin, Texas

PREFACE

This is the final report under Contract DA 19-129-QM-1383, which was initiated March 26, 1959 and terminated September 30, 1962. The extent of the activity carried on under this contract is not entirely indicated by the 17 formal reports and 9 memorandum reports which have been issued. The program has contributed significantly to the graduate program in the Departments of Civil Engineering and Engineering Mechanics at The University of Texas. Six Master's theses have been written on various aspects of the aerial-delivery problem, and two Doctoral dissertations now under preparation also had their inceptions in this program. In addition, numerous graduate and undergraduate students who did not write theses have been supported by this program.

Another activity which should not go unmentioned is the Aerial Delivery Conference held at The University of Texas' Balcones Research Center June 23 and 24, 1959. This conference brought together 29 people from various parts of the country, each interested in the problems of aerial delivery. These men were able to exchange ideas and observe first hand how effectively vehicles can be cushioned for aerial delivery. The entire program of aerial delivery was given an effective boost by this conference.

On behalf of the entire staff of the laboratory and of the many students who have been trained in the methods of engineering research while being supported by this contract, I express our sincere appreciation

to the Quartermaster Research and Engineering Command. We also gratefully acknowledge the support and cooperation we have received from Mr. Harold L. Jones and Mr. Harry L. Freeman. Without their contributions this program could not have been carried on.

Directing Staff:

J. Neils Thompson, Director and Professor of Civil Engineering

E. A. Ripperger, Associate Director and Professor of Engineering Mechanics

Charles Ford, Research Engineer (Faculty) and Instructor, Engineering Mechanics Department

Michael Reifel, Research Engineer (Faculty) and Instructor, Engineering Mechanics Department

J. Neils Thompson, Director
Structural Mechanics Research Laboratory
The University of Texas
Austin, Texas

October 26, 1962

TABLE OF CONTENTS

TABLE OF CONTENTS
(Cont'd)

LIST OF FIGURES

LIST OF FIGURES
(Cont'd)

LIST OF TABLES

ABSTRACT

All of the investigations completed under Contract DA 19-129-QM-1383 are summarized. This includes studies of cushioning materials, analyses of mathematical models which are pertinent to the problem of aerial delivery, studies of the reactions of specific vehicles to impact loading, and the cushioning "handbook" in which the state of the art of cushioning for aerial delivery is presented.

A bibliography of all reports issued under this contract is included.

INTRODUCTION

Work on this contract was initiated March 26, 1959, and continued at a varying level of activity until termination of the contract September 30, 1962. During this period, 17 formal reports, not including the bimonthly interim reports, have been issued. The purpose of this, the final report, will be to summarize in a very brief fashion the objectives of the investigation and the accomplishments reflected in the 17 reports.

This contract was set up and funded initially in three separate and distinct but related parts which are referred to as Phase I, Phase II, and Phase III. Later, a fourth part, referred to as Phase IV, was added. The summary which follows will be by phases.

PHASE I

Research Evaluation of Materials for Energy Dissipation

In this phase, the force-deformation characteristics and energy-dissipating capabilities of selected materials and systems were determined, particularly with regard to the effects on these properties of such factors as rate of loading, environmental conditions, and geometry of specimen. Materials and systems to be studied were selected by the contracting officer. These included Air Bags, Foamed Plastics, and Paper Honeycomb. During intervals between investigations, the technique for making the required measurements was studied and improvements were developed. This type of development has progressed to the point now where the slide-wire technique for displacement measurements and the force-plate technique for force measurements have been abandoned. In the new method for obtaining dynamic stress-strain curves for crushable cushioning materials, the sample of the material under study is placed on a heavy reinforced concrete block. A suitable mass is then dropped on the sample. The acceleration of the mass as sensed by a fluid-damped accelerometer is recorded as a function of time. In addition, the velocity of impact is recorded. The acceleration and impact velocity are then fed into an analog computer which performs the necessary integrations, additions, subtractions and scale changes, and then plots out the stress-strain curve. Difficulties with trailing wires are eliminated by telemetering the acceleration to the recording station. An extremely small and rugged

transmitter does the telemetering. With this system, force-displacement measurements in any direction can be obtained. This greatly facilitates the study of cushioning characteristics particularly where horizontal components of velocity are involved.

Specific studies undertaken under Phase I are indicated by the titles of the following reports.

Energy Dissipating Characteristics of Air Bags

This report describes the results of an experimental study of three types of airbag devices. Typical curves are presented which show the variation of internal pressure, and mass acceleration with both time and displacement. Some of these curves are shown in Fig. 1. The airbags investigated were found to be capable under suitable conditions, of dissipating up to 18,000 ft lb of energy at an impact velocity of 35 ft/second. The performance was somewhat inconsistent, however.

High-Velocity Impact Cushioning, Part VI, 108C and 100C Foamed Plastics

These were experimental rigid polyurethane plastics fabricated by the Atlantic Research Corporation for the Quartermaster Research and Engineering Command. The objective of the program was the determination of stress-strain characteristics and energy dissipation of these plastics as a function of

1. Material density
2. Impact velocity
3. Impacting mass
4. Impact energy
5. Temperature
6. Pad thickness

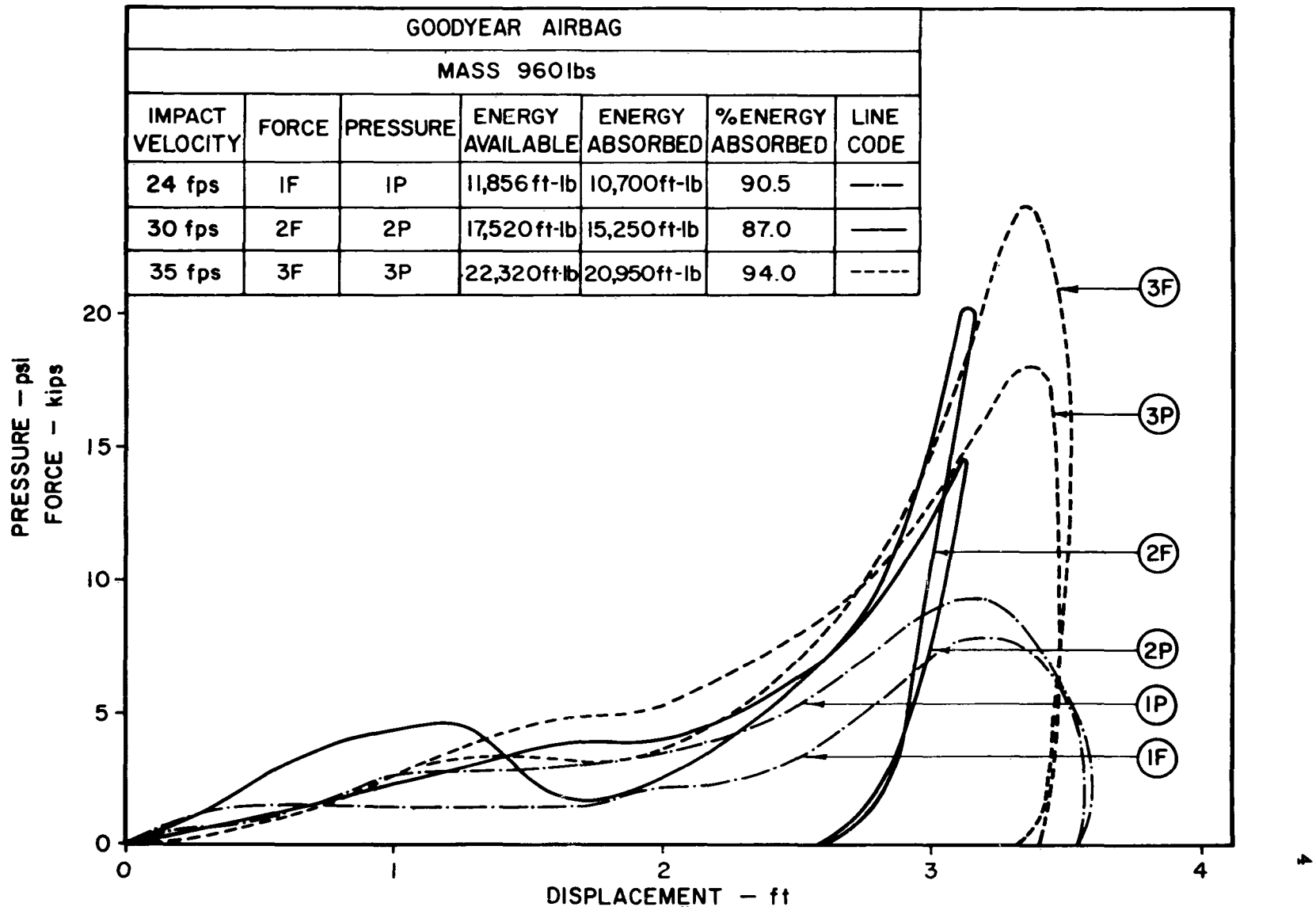

Fig. 1. Force and Pressure vs Displacement. Goodyear Airbags.

Typical stress-strain curves for the 108C are shown in Fig. 2. The 100C has virtually the same characteristics. These foamed plastics are relatively insensitive to environment. For example the stress-strain curves obtained at 85F and -12F differ very little. The material is somewhat brittle, however, on impact and tends to blow out so that when the mass strikes, large pieces of material are expelled from the specimen uncrushed.

Impact Tests of a Rigid Polyurethane Foam

This was a study of a rigid freon-blown polyurethane foam which was also an experimental material. At 80 per cent strain, this material dissipated approximately 5000 ft-lb of energy per cubic foot and had an average crushing stress of 6500 lb/ft^2. Paper honeycomb (80-0-1/2), it might be noted, dissipates at 70 per cent strain about 4000 ft lb/ft^3 and has an average crushing stress of about 5900 lb/ft^2. Obviously, the foamed plastic, except for its greater insensitivity to environment, and its greater homogeneity is not significantly better as a cushioning material than paper honeycomb.

Energy Dissipation Characteristics of Foamed Plastics

The plastic in this study was also a freon-blown rigid polyurethane. In this case, however, the specimens were faced with 60 lb kraft paper to help reduce the blowout referred to above. There was no really significant difference between the properties of this material and those of the foam discussed above.

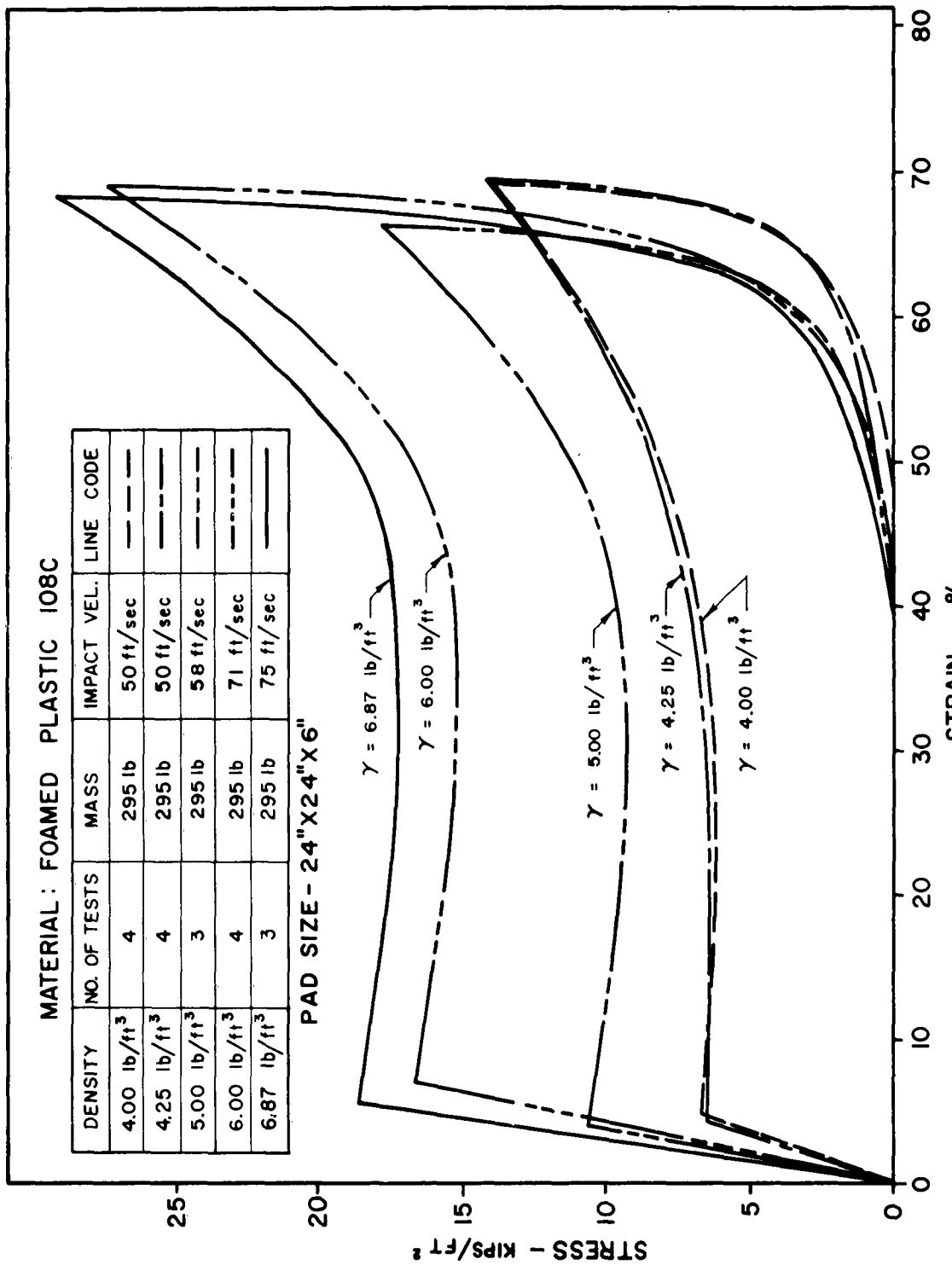

Fig. 2. Effect of Density on the Stress-Strain Curve for Foamed Plastic 108C.

PHASE II

Research on the Resistance of Complex Structures to Shock and on the Establishment of Indices for "Shock Ratings"

The approach to this phase of the aerial-delivery studies has been to start with a simple undamped spring-mass system and consider the effects of applied pulse shape, pulse duration, and maximum pulse amplitude on the displacement of the mass. The pulse referred to is an acceleration pulse applied to the point of support for the system. As the understanding of this simple system and its reaction to impulsive loading increased, more complex systems were considered. The more complex systems included (1) the single-degree-of-freedom system with damping, (2) the undamped two-degree-of-freedom system, (3) a yielding one-degree-of-freedom system without damping, (4) a damped, yielding one-degree-of-freedom system, and (5) a multiple-degree-of-freedom system.

This approach to the problem of fragility or "shock rating" is based upon two major assumptions. (1) Although a vehicle has an infinite number of degrees of freedom these can be reduced for practical purposes to a few essential degrees of freedom. In the design of a cushioning system, perhaps two degrees will be sufficient, but for improvements in the design of a vehicle more degrees of freedom may be required in the analyses. (2) The characteristics which produce the largest displacements in a given system whether they are inherent in the system or in the applied pulse are the best indicators of damage possibilities.

Damages sustained by vehicles in actual drops have been observed to be progressive in nature. After the first drop, very little damage can be detected. After the second drop, only a little more damage can be observed. Finally after many drops, enough damage has accumulated to make it obvious even to a casual inspection. It has not been possible to associate the damage observed with any of the characteristics of the applied pulse or any of the other pertinent features of the drop. Thus it appears that it may not be possible to specify a "shock rating" for a vehicle in any but the vaguest terms. Nevertheless, further studies and analyses of the response of complex structures to impulsive loading are necessary if the design of cushioning systems and of vehicles that are to be air delivered is to proceed in a rational manner instead of by trail and error. The various programs of investigation and the conclusions reached are summarized below.

Single-Degree-of-Freedom, Undamped System

This problem has been rather thoroughly studied by other investigators in the past. Hence it was only necessary to search the existing literature. This search revealed that

1. For small values of the ratio of pulse duration to the period of the system $\frac{t}{T} < 0.25$ the response of the system is determined only by the applied impulse. That is, for a given pulse duration and $\frac{t}{T}$ less than 0.25, the response is determined essentially by the amplitude of the pulse.

2. For values of $\frac{t}{T}$ greater than $\frac{1}{4}$, the response is determined by pulse shape, pulse duration, and pulse amplitude.

The periods of vibrations of basic components of vehicles which have been studied, and the observed durations of impacts of dropped vehicles are such that typical values of $\frac{t}{T}$ appear to be less than $\frac{1}{4}$. Enough information is available concerning the response of a single-degree-of-freedom system in this range to indicate that further study in this area is unnecessary. On the other hand, very little information is available concerning the response of a single-degree-of-freedom, damped system, or of multiple-degree-of-freedom systems with or without damping.

The Single-Degree-of-Freedom System with Viscous Damping

In this study, six differently shaped acceleration pulses were applied to the system. The response of the system to each of these various pulses was determined and presented in the form of displacement and acceleration shock spectra. Typical results are shown in Figs. 3 and 4. These results indicate a significant reduction in the maximum response, whether displacement or acceleration, with increasing damping. A substantial reduction in the maximum response is accompanied of course by a substantial reduction in the stress induced by the impact in the elastic element of the system.

The results of this study lead to the conclusions that pulse shape

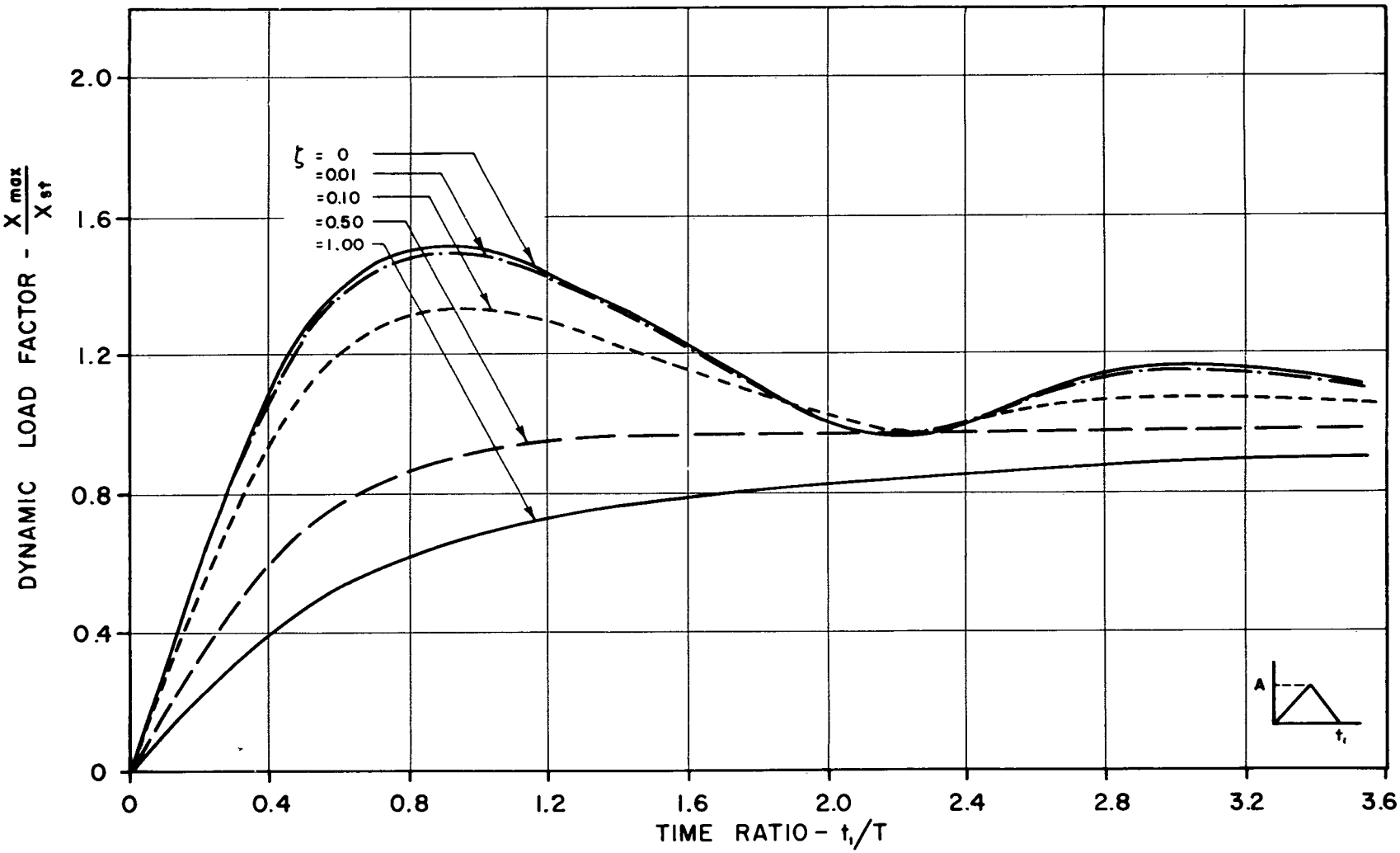

Fig. 3. Displacement Shock Spectrum for Triangular Pulse II
One Degree of Freedom

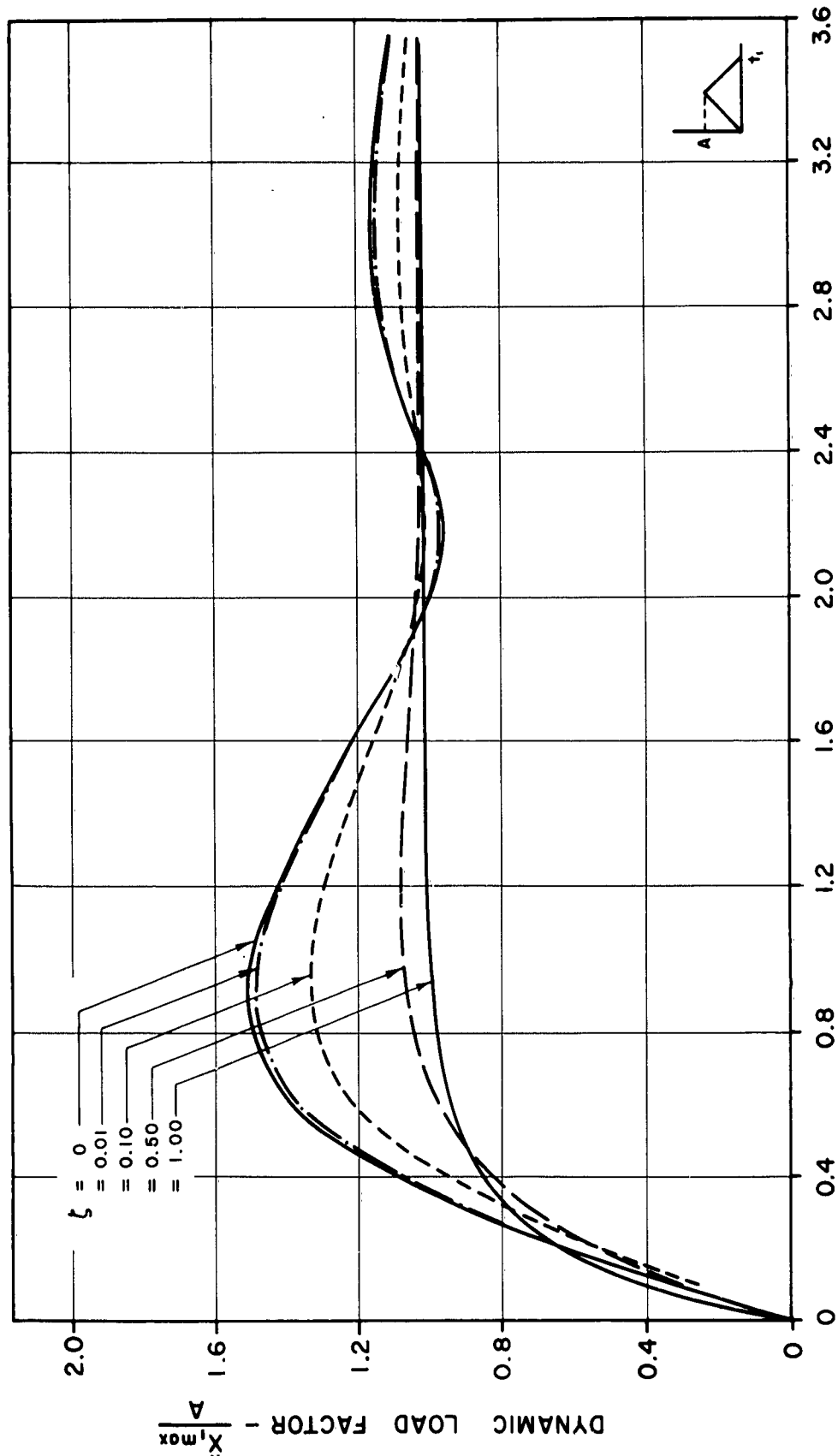

Fig. 4. Acceleration Shock Spectrum for Triangular Pulse II
One Degree of Freedom

has little effect on the response of the system when the time ratio $\frac{t_1}{T}$ is less than 0.2, and that for $\frac{t_1}{T} > 0.2$, the most significant characteristic of the pulse shape is the rise time. (Here t_1 is the duration of the pulse as shown in Fig. 3.) The dynamic load factor is not a function of pulse amplitude or total impulse. The dynamic load factor is defined here as the ratio of maximum displacement to the statical displacement of the spring under the loading of the mass of the system, or as the ratio of the maximum acceleration produced to the maximum acceleration applied.

The Response of a Two-Degree-of-Freedom Undamped System Subjected to Impulsive Loading

The same six acceleration pulses used in the single-degree-of-freedom studies were applied to a two-degree-of-freedom system. Two additional parameters are introduced to simplify the presentation of results. These parameters are

1. The ratio of the two masses in the system
2. The ratio of the two spring constants.

Typical shock spectra for the two-degree-of-freedom system are shown in Figs. 5, 6, 7, and 8. In these figures x_1 and x_2 are the displacements of the two masses and x_a and x_b represent the compression of the two springs. A sketch of the system and of the applied pulse is shown in Fig. 5. The results of this investigation show that for all mass ratios considered with $\frac{K_2}{K_1} > 2.0$, the response is essentially the same as that of a one-degree-of-freedom system subjected to the same impact conditions. This indicates that if the spring between M_1 and M_2 is stiff enough in

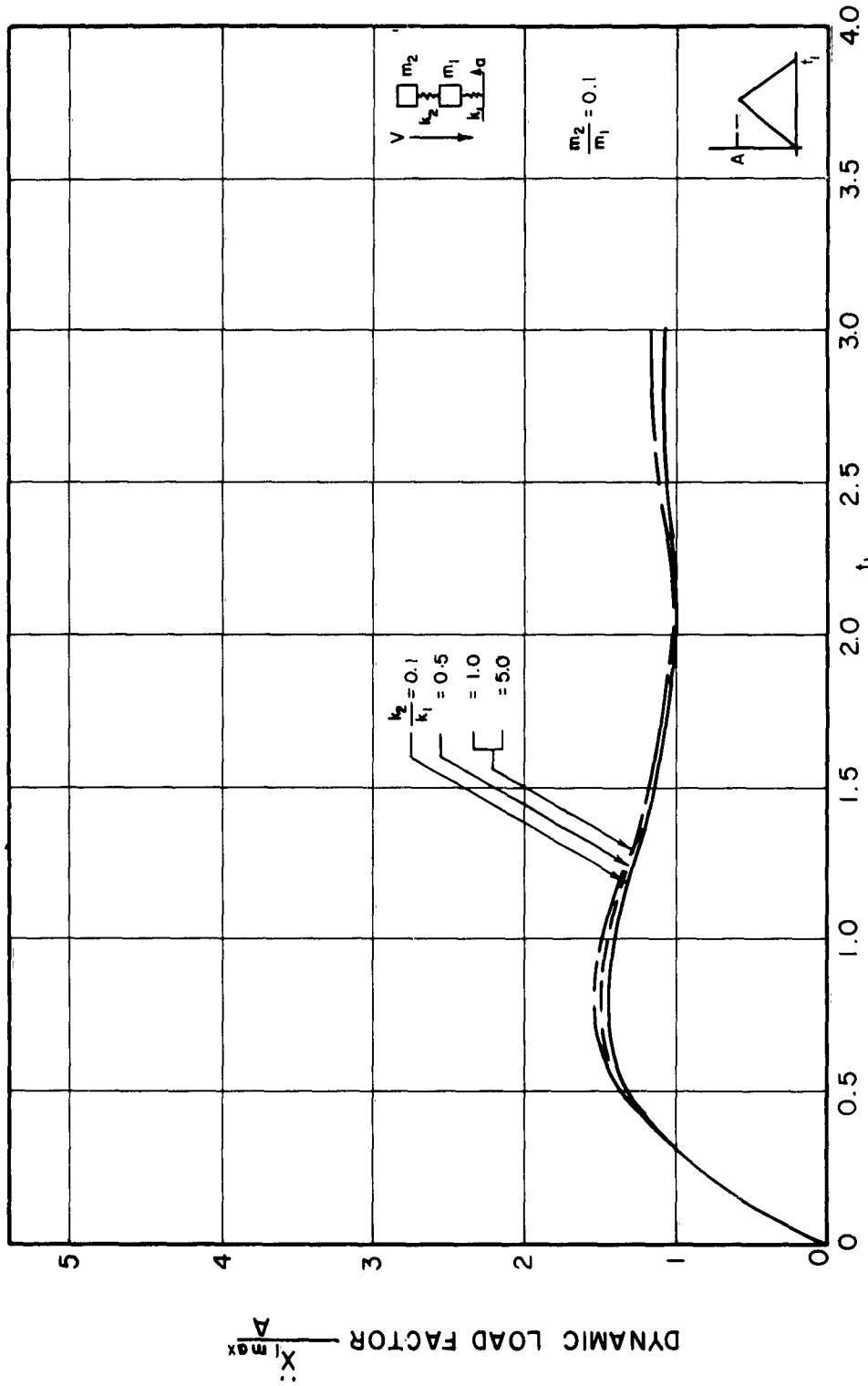

Fig. 5. Acceleration Shock Spectrum for Triangular Pulse II
Two Degrees of Freedom

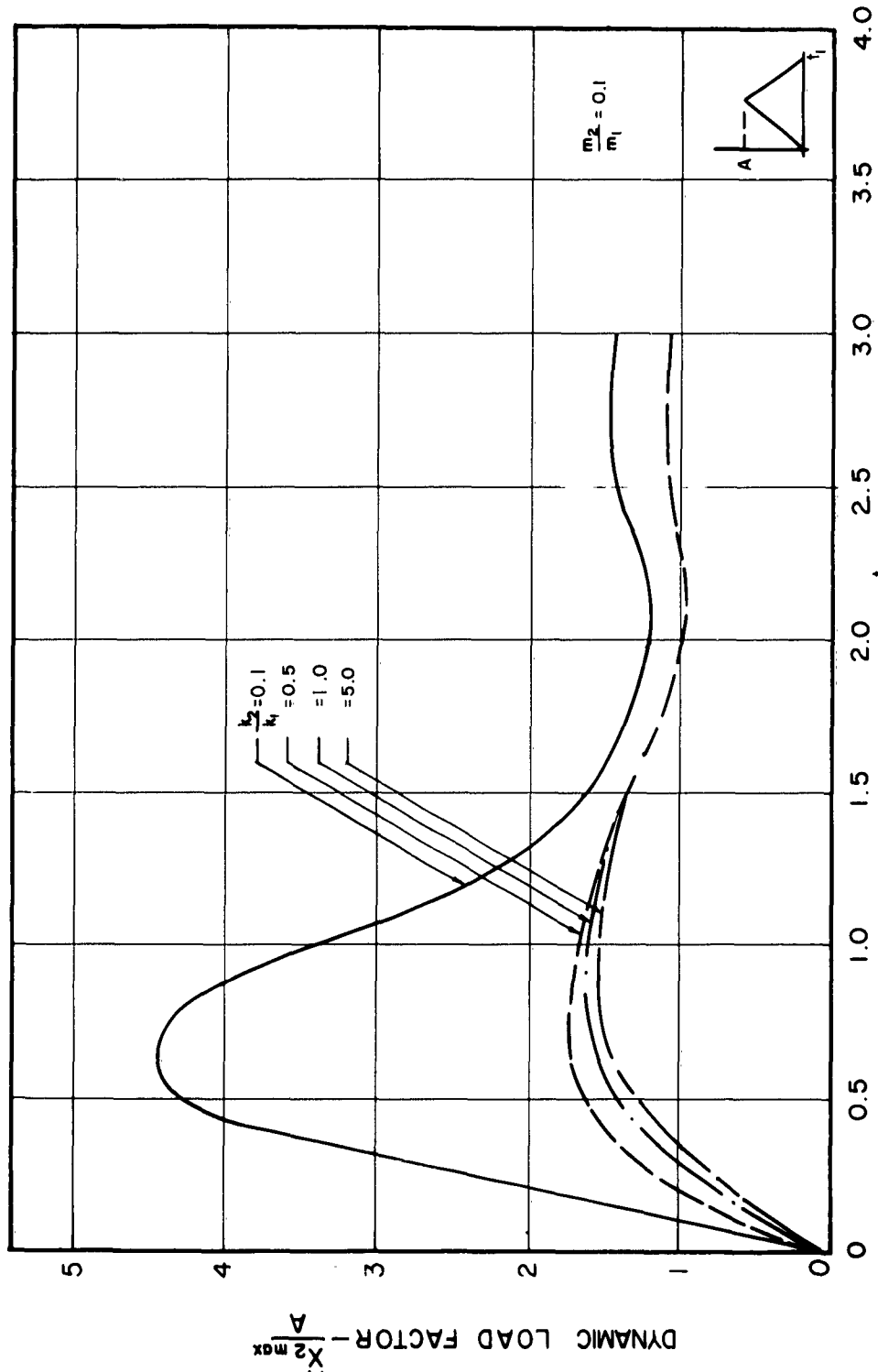

Fig. 6. Acceleration Shock Spectrum for Triangular Pulse II
Two Degrees of Freedom

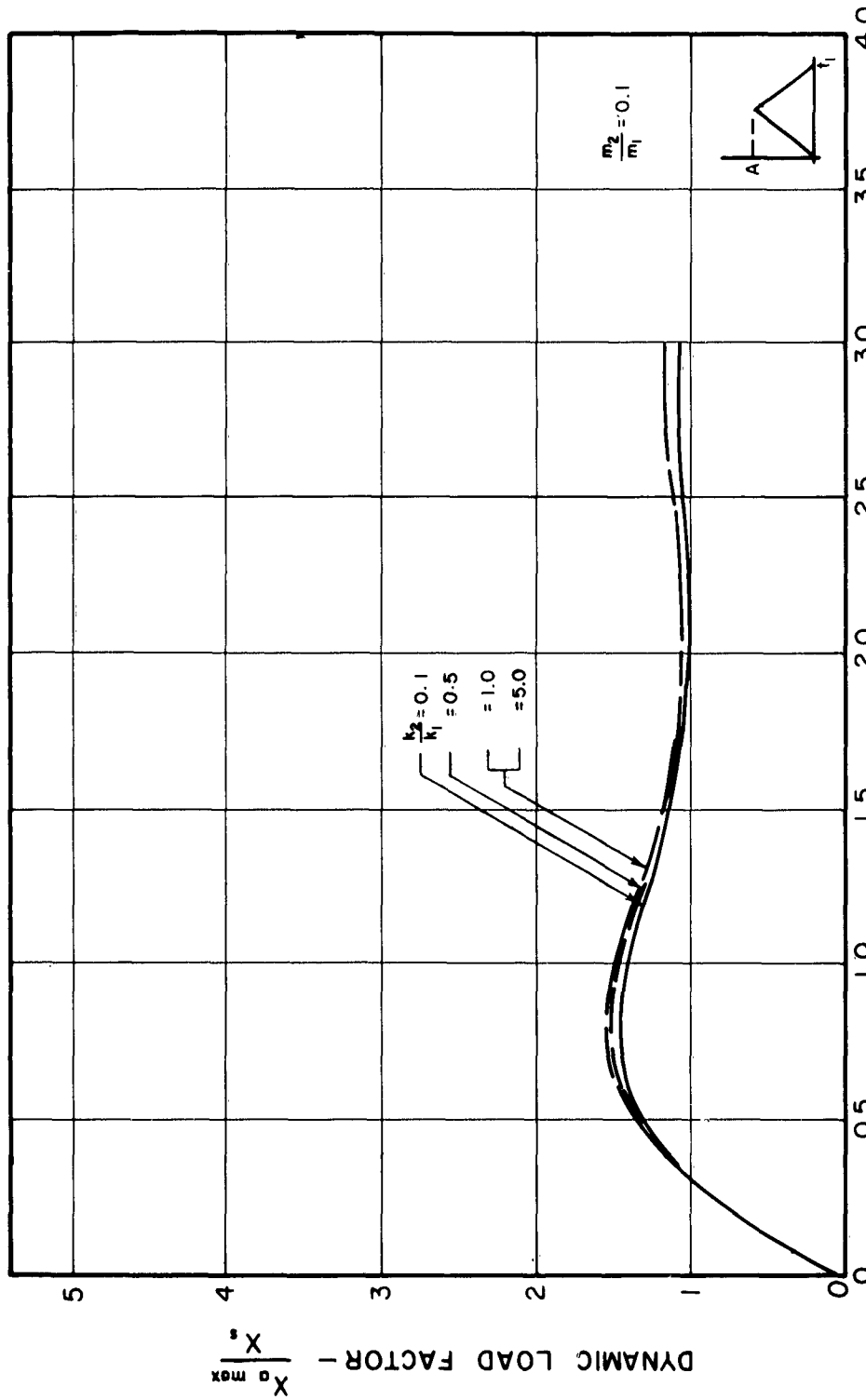

Fig. 7. Displacement Shock Spectrum for Triangular Pulse II Two Degrees of Freedom

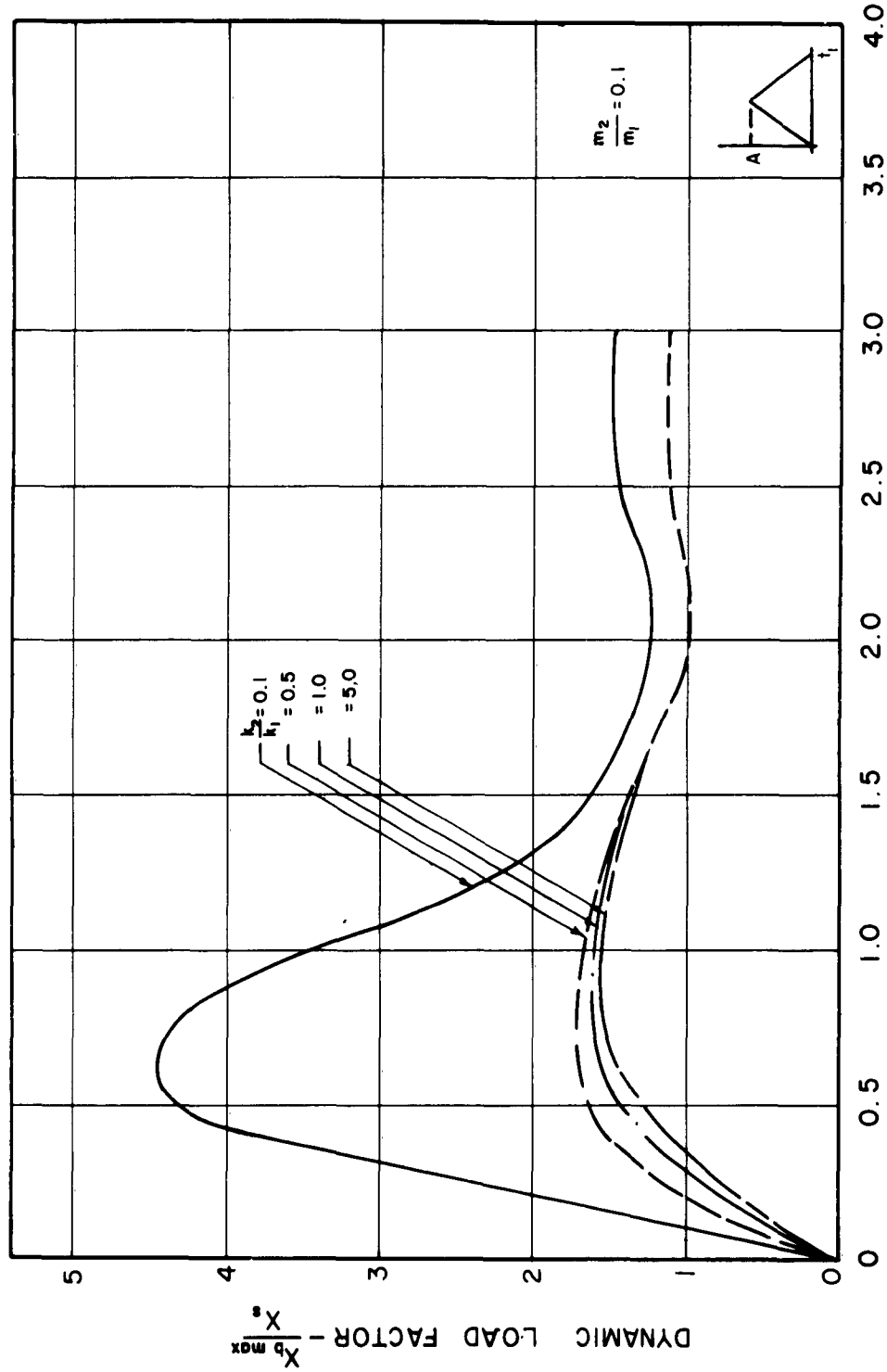

Fig. 8. Displacement Shock Spectrum for Triangular Pulse II
Two Degrees of Freedom

comparison to the spring between M_1 and the support, the two-degree-of-freedom system is, at the frequencies of excitation involved, practically a one-degree-of-freedom system. If the lower of the two coupled natural periods of the system is designated as T_1, the ratio $\frac{t_1}{T_1}$ becomes a useful parameter. If $\frac{t_1}{T_1} < 0.3$, pulse shape has little effect on system response; and for $\frac{t_1}{T_1} > 0.3$, pulse rise time is the most significant characteristic of pulse shape. The dynamic load factor defined in terms of the response of either mass is not a function of pulse amplitude or total impulse, but actual deflection and acceleration do depend on these parameters.

Plastic Deformation of a Single-Degree-of-Freedom System Subjected to Impulsive Loading

In the previous studies of linear systems, the amplitude of the response was selected somewhat arbitrarily as the most significant quantity in the prediction of damage because observed damage to dropped vehicles has generally been of the permanent-set type. It seems reasonable to assume that those conditions which produce maximum deflection in an idealized linear system will also produce maximum permanent deformation in a yielding system. This assumption requires some verification however, The investigation to be summarized now represents an attempt to determine the validity of that assumption. A simple low-carbon, steel beam supported at the middle and loaded at the ends with the tip masses was chosen to represent a single-degree-of-freedom system with a yielding spring. The beam, it may be seen, actually consists of two independent cantilevers with tip masses.

Accelerations were applied to the roots of these cantilevers by dropping a large mass to which the cantilever assembly was attached on a suitable cushion. Variations in the pulse shape, amplitude, and duration of the applied acceleration were produced by changing the dimensions and properties of the cushioning. It proved to be quite difficult to produce, by this method, the pulse shapes desired, and to control the durations and amplitudes. As a consequence, the results of the study were not conclusive. A typical acceleration pulse is shown in Fig. 9. Permanent deflection produced in the tip-loaded cantilever beams by application of a pulse of this form are shown in terms of nondimensional parameters in Fig. 10. The symbols which appear in Fig. 10 are defined as follows. A is the peak acceleration applied, T is the natural period of the system, t is the duration of the pulse, L is the length of the beam, δ is the permanent deflection and δ_y is the yield deformation.

Due to the difficulty experienced in controlling the applied pulse, the individual effects of pulse shape, $\frac{t}{T}$, and impulse could not be isolated.

As a consequence of the experimental difficulties encountered, some further theoretical studies were initiated to determine the extent to which the parameters controlling permanent deformation of a yielding system subjected to impulsive loading can be isolated and studied. Two reports on these studies have been written. They are summarized as follows.

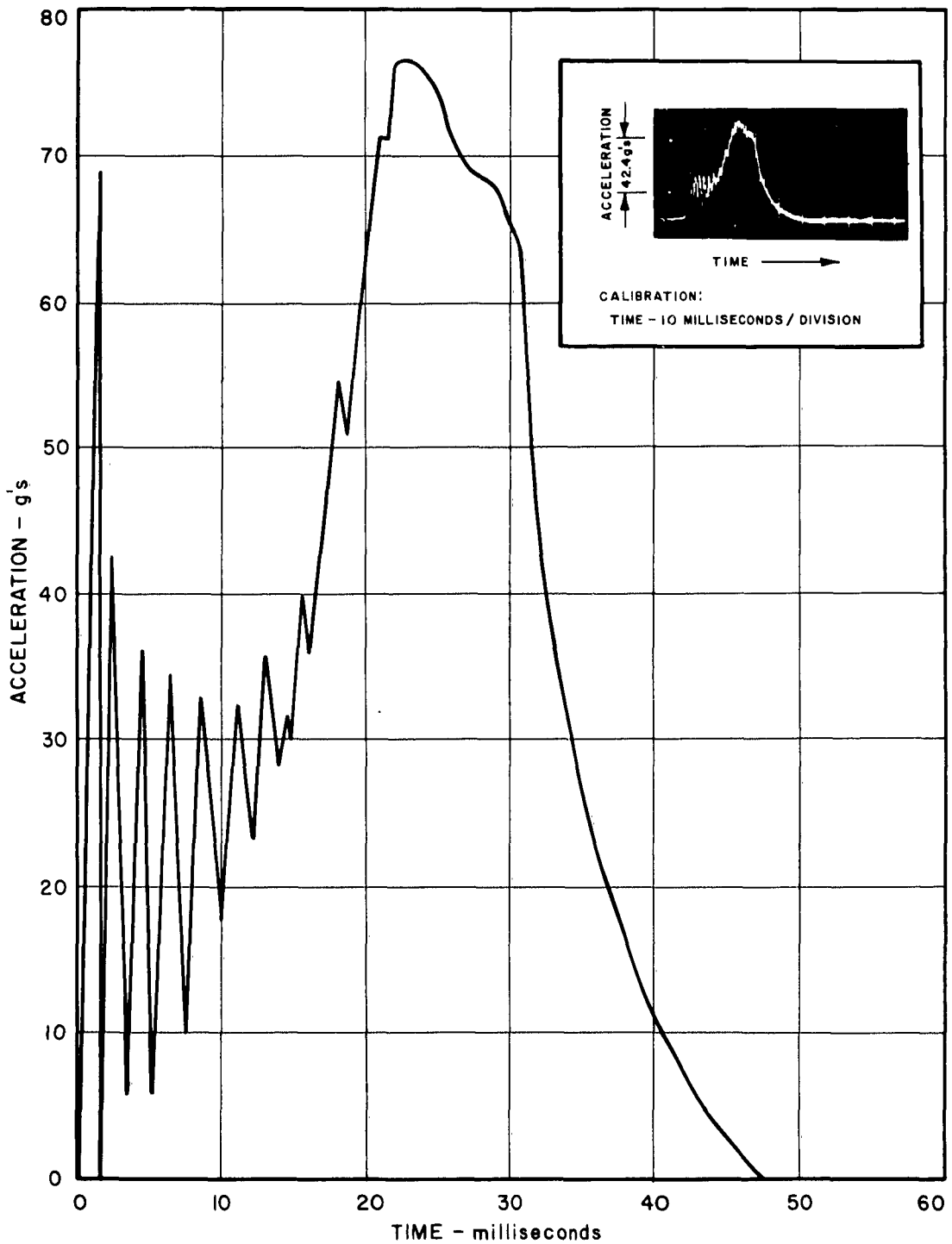

Fig. 9. Oscilloscope Record of Acceleration Pulse

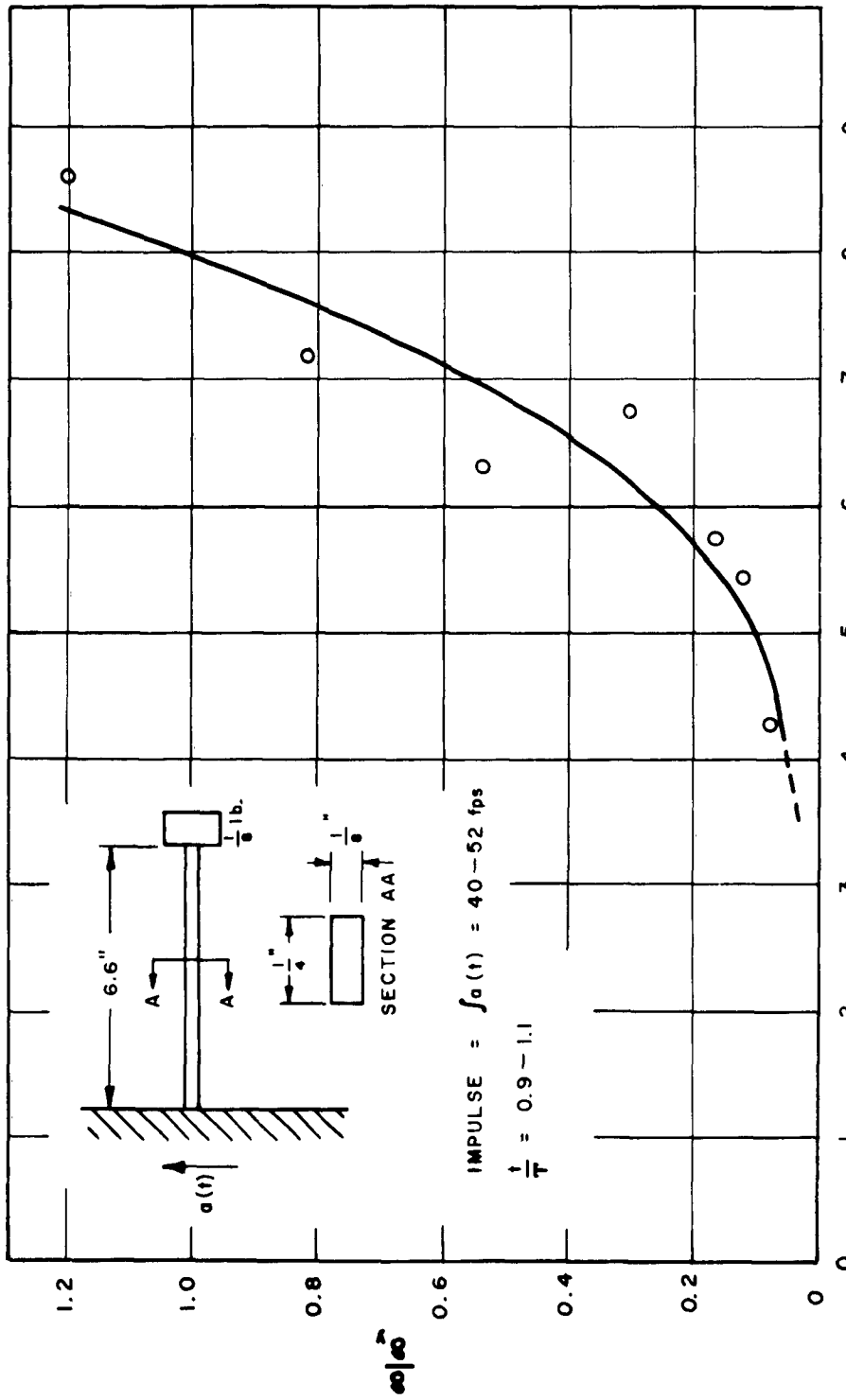

Fig. 10. Permanent Tip Deflection of Mild Steel Cantilever Beam Accelerated at the Root.

An Analytical Study of an Undamped Nonlinear Single-Degree-of-Freedom System Subjected to Impulsive Loading

In this study, the same tip-loaded cantilever beam of mild steel used in the previous study was the model. Equations of motion for the tip mass were written and solved assuming that the static load deflection curve for the beam also represented its dynamic behavior. This means that during unloading the beam deflection follows a straight line parallel to the initial portion of the load deflection curve. Upon reloading after unloading the curve retraces the unloading portion until the original curve is reached. Deflection then follows the original curve unless unloading again occurs. This behavior is illustrated in Fig. 11. To study the effect of various pulse parameters on the permanent deformation of the beam, 16 different input pulse shapes were included in the computations. It was found that the ratio of the rise time of the pulse to the natural period of the system is quite significant in determining the permanent deformation in the case of triangular pulses.

A nondimensional representation of the calculated permanent deflection produced by three different pulse shapes is shown in Fig. 12. Also, some experimental results obtained by using a Hyge accelerator are shown. The number of parameters which affect permanent deformation is too large to permit an adequate representation of the relationship in a two-dimensional plot. Consequently, a three-dimensional plot illustrated in Fig. 13 has been used. This plot shows clearly that there are combinations of the parameters which produce permanent deformation, while other combinations in which some of the individual parameters are not changed do not produce deformation. For example,

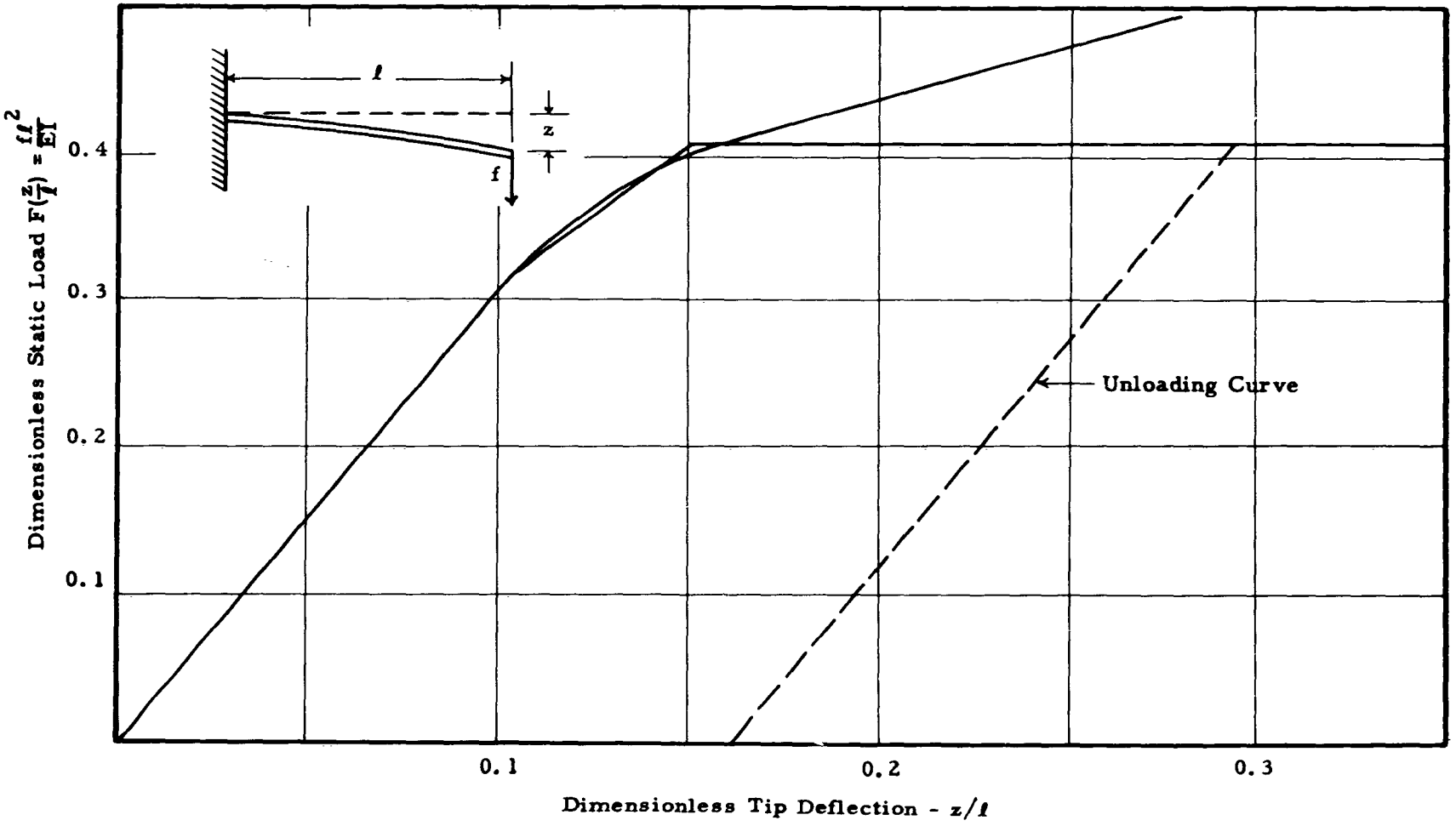

Fig. 11. Dimensionless Static Load $F(\frac{z}{l})$ Versus Dimensionless Tip Deflection z/l for a Mild Steel Cantilever and Corresponding Straight Line Approximation

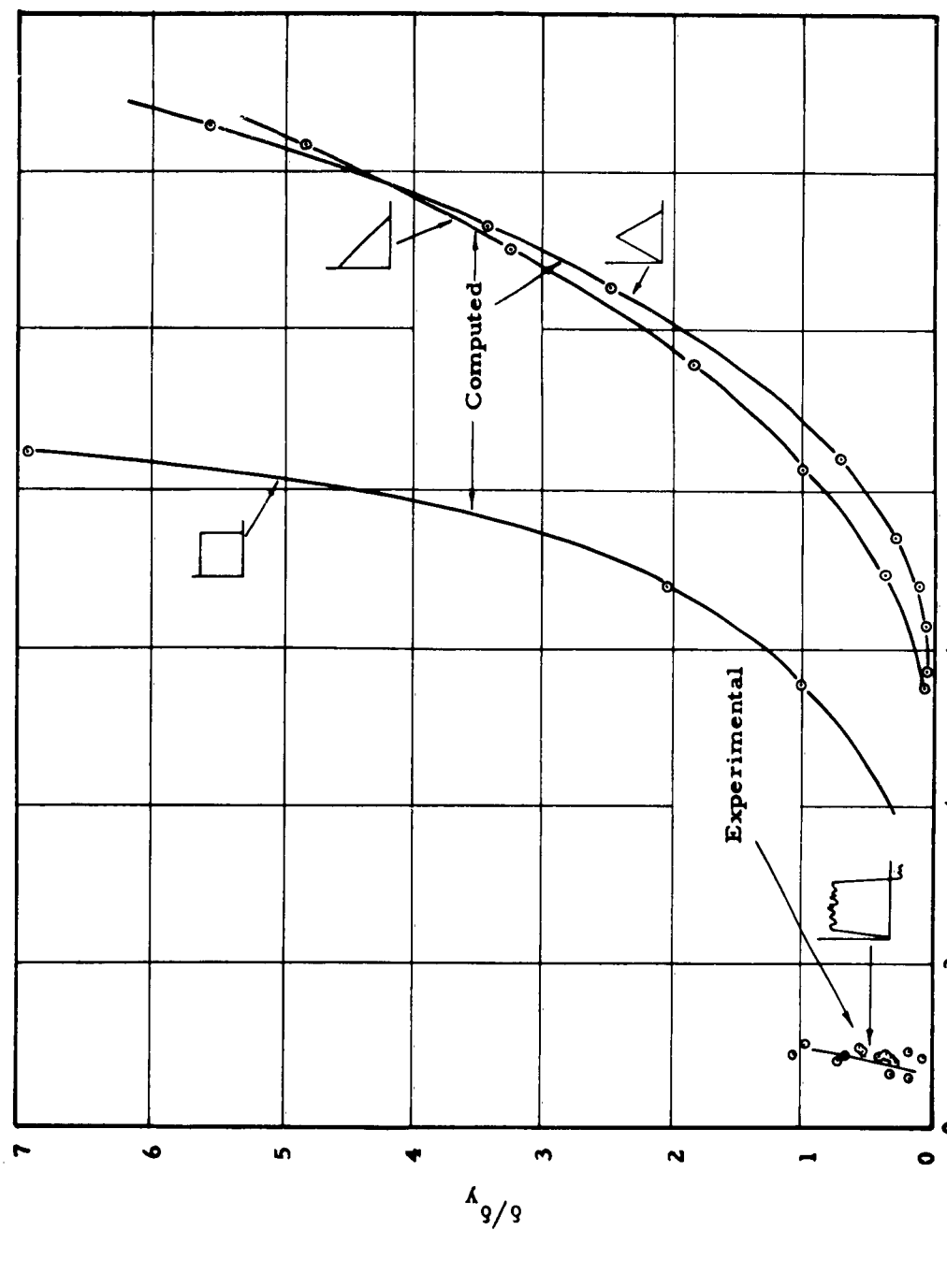

Fig. 12. Permanent Deformation Produced by Three Acceleration Pulses

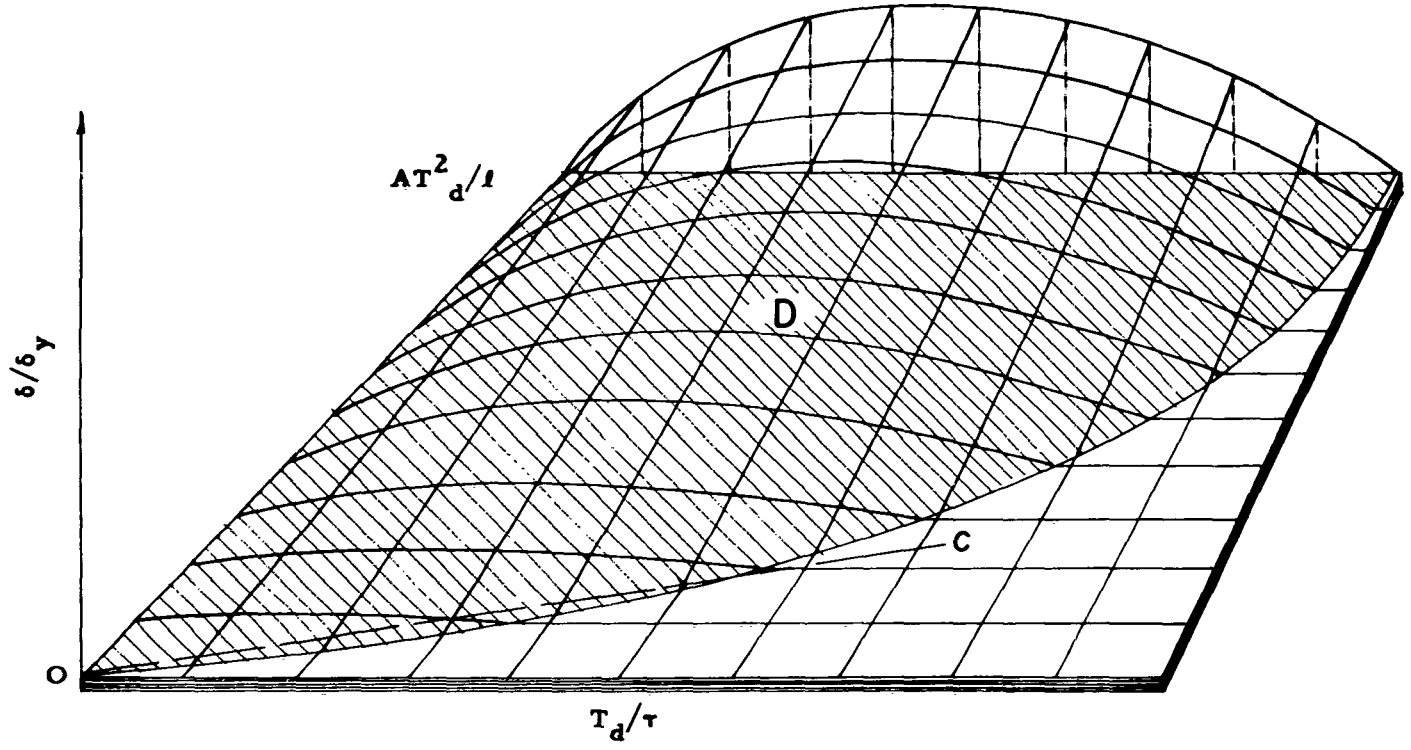

Fig. 13. A Hypothetical Surface which Illustrates the Functional Relationship Between Pulse Duration, Pulse Amplitude, and Natural Period of the Beam

if T_d/τ is very large, AT_d^2/ℓ must be very large to produce any permanent deformation. Two-dimensional plots, such as the one shown in Fig. 12, actually represent a cross section through the three dimensional plot. From the three-dimensional representation, it is easily seen that a part of the boundary of the surface in the T_d/τ - AT_d^2/ℓ plane is essentially a straight line. This is believed to be at least a partial explanation of some of the past experimental results in which vehicles were subjected to larger and larger accelerations without any appreciable damage occurring. In this past work, the amplitude of acceleration has been considered the most important parameter and investigations were planned accordingly. To determine the maximum acceleration allowable for a given vehicle, accelerations were gradually increased, but since the impact velocity remained constant, T_d, the impact duration, was decreased as the acceleration increased. It was observed that even though acceleration was increased by a factor of four, no damage was observed. This puzzling observation can be explained by reference to Fig. 13, and to the fact that for a rectangular acceleration pulse $AT_d = V$, where V is the impact velocity. With V as a constant, the relationship between AT_d^2/ℓ and T_d/τ is a straight line such as OC in Fig. 13. Obviously, for any cushioning configuration which follows a curve such as OC, an increase in acceleration amplitude will not produce any appreciable permanent deformation.

Experimental studies have confirmed the general shape of the boundary line between the region of no permanent deformation, and the

region in which permanent deformation occurs in the T_d/τ - AT_d^2/ℓ plane. In these studies parameters were varied in such a way that points near the boundary, in both the elastic and plastic regions, were obtained. Starting in the elastic (no permanent deformation) region, points were obtained near the boundary. For the next test, the parameters were changed so as to move the point a little nearer the boundary. As soon as the boundary was crossed, as indicated by permanent deformation, the parameters were changed and the entire process repeated so as to cross the boundary at another point. The results of these experiments are shown in Fig. 14. These results were obtained using a Hyge acceleration producing half-sine-wave pulses. The acceleration amplitude, A, ranged from 17.1 to 153g, and the duration T_d ranged from 5.4 to 44.9 milliseconds. Variations in the natural frequency of the beam were produced by changing the beam length and the tip weight.

Conclusions based on the results of this study are as follows.

1. If it is possible to define a rise time, t_r, for a pulse, maximum permanent deformation may be expected when t_r/τ has a value near 1/4.

2. The shape of the acceleration pulse, in general, has a marked effect on permanent deformation. Among the 16 pulses studied, the extremes in permanent deformation varied by a factor of 45.6.

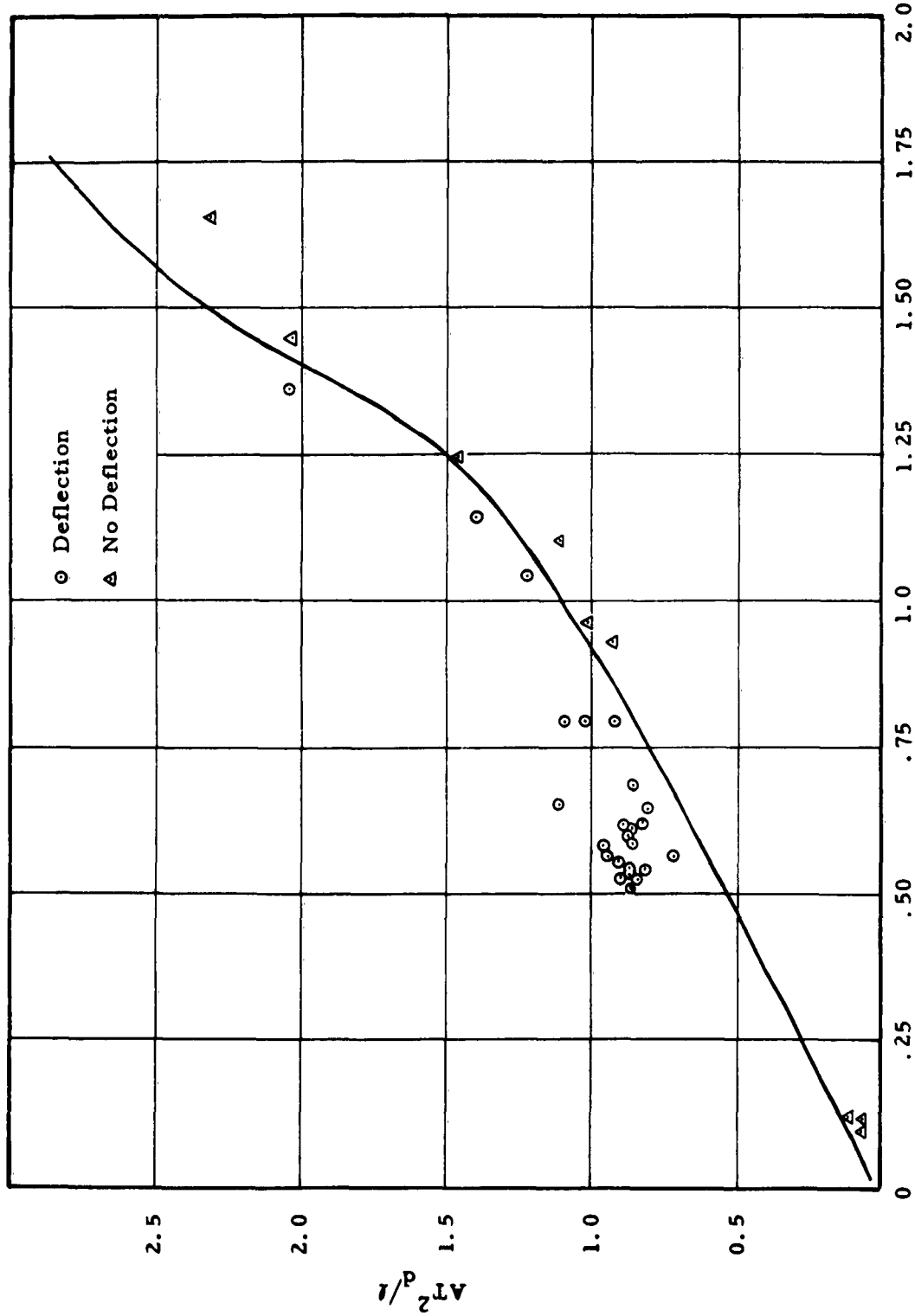

Fig. 14. Boundary Between Deflection and No Deflection Regions

3. The effects of A, T_d and ℓ cannot be separated (ℓ is the length of the beam). But for a given pulse shape and a given beam (i.e. τ and ℓ constant) the permanent deformation increases as either A or T_d increases, after a certain minimum value of A is exceeded.

4. Experimental results support the theoretical conclusions.

5. The two parameters AT_d^2/ℓ and T_d/τ seem to be the most significant in determining the permanent deformation a given pulse will produce.

The Effects of Acceleration Pulse Parameters on the Permanent Deformation of a Damped Single-Degree-of-Freedom System

If the energy which produces the permanent deformation in a system which is impulsively loaded is initially stored in the system, and therefore limited in magnitude, any dissipation of this energy by damping should reduce the permanent deformation produced. The question is, can a significant reduction in permanent deformation be accomplished with damping in the order of magnitude to be expected in vehicle parts? The objective of this study was to determine to what extent the conclusions reached in the study of the undamped system might be modified by damping.

In this study, it was again found to be necessary to represent the relationship between the permanent deflection and the various parameters in a three-dimensional plot. The plot is actually a surface which is

referred to here as the shock surface. The shock surface for a rectangular pulse is illustrated in Fig. 15. In this representation, the parameters are changed somewhat from those shown in Fig. 13. These parameters are chosen so that for each value of the damping factor, ζ, a different surface will be produced. In this illustrative example $\delta/\delta_{y\ell}$ is the ratio of permanent deformation to the yield deformation, T_d/τ is the pulse duration divided by the natural period of the system and $Am/F_{y\ell}$ is the pulse amplitude multiplied by the mass of the system divided by the force required to produce yielding under static conditions. The effect of damping is illustrated by Fig. 16. As indicated in the caption, the two curves are actually cross sections from a family of surfaces such as the one in Fig. 15. Obviously, damping has a very significant effect on the permanent deformation produced by a given pulse. The effect diminishes, however, as the damping increases, i. e., an increase in the damping factor, ζ, from 0 to 0. 1 produces a greater reduction in permanent deformation than an increase from 0. 5 to 0. 6.

If the boundary between the elastic and the plastic region as represented by the shock surface in Fig. 15 is referred to as the base line, the effect of damping can be further illustrated by showing how the base line is altered by changes in the damping constant. Base lines for three different damping factors are shown in Fig. 17. It may be seen that a system with a damping factor $\zeta = 0.8$ requires almost twice

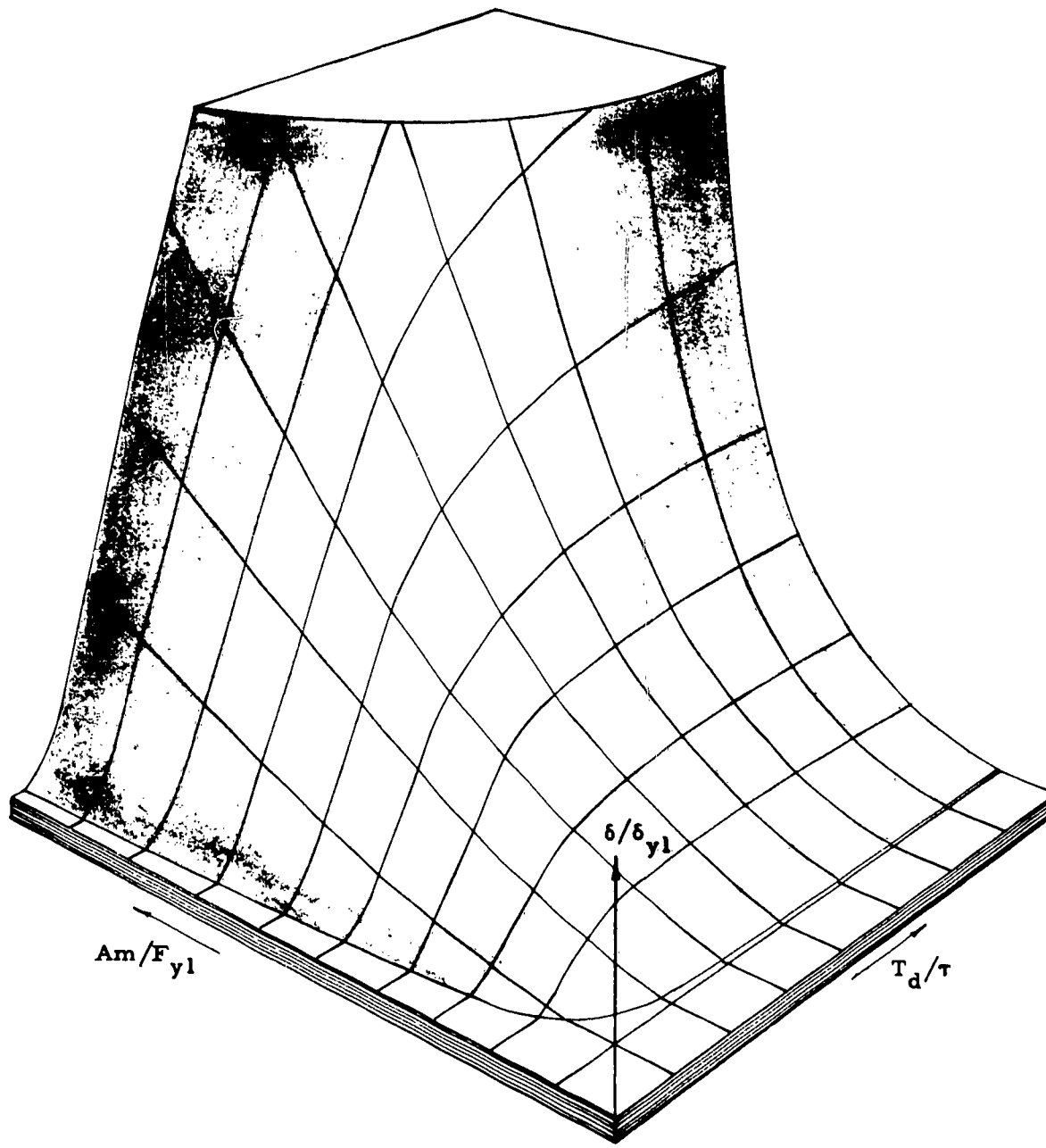

Fig. 15. Shock Surface for Rectangular Pulse, $\zeta = 0.1$

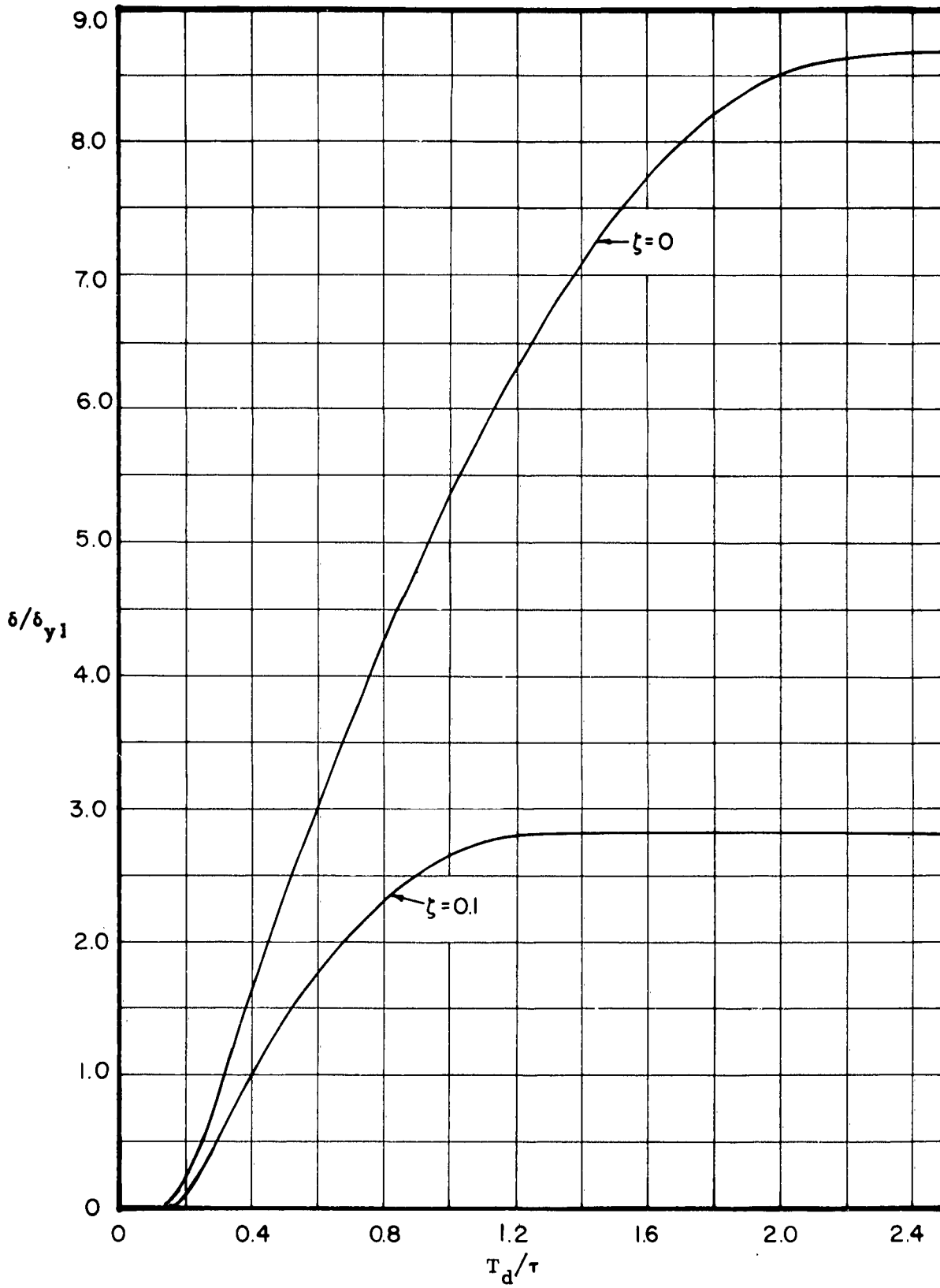

Fig. 16. Cross Sections of Two Shock Surfaces for Rectangular Pulse with $Am/F_{y1} = 1.212$

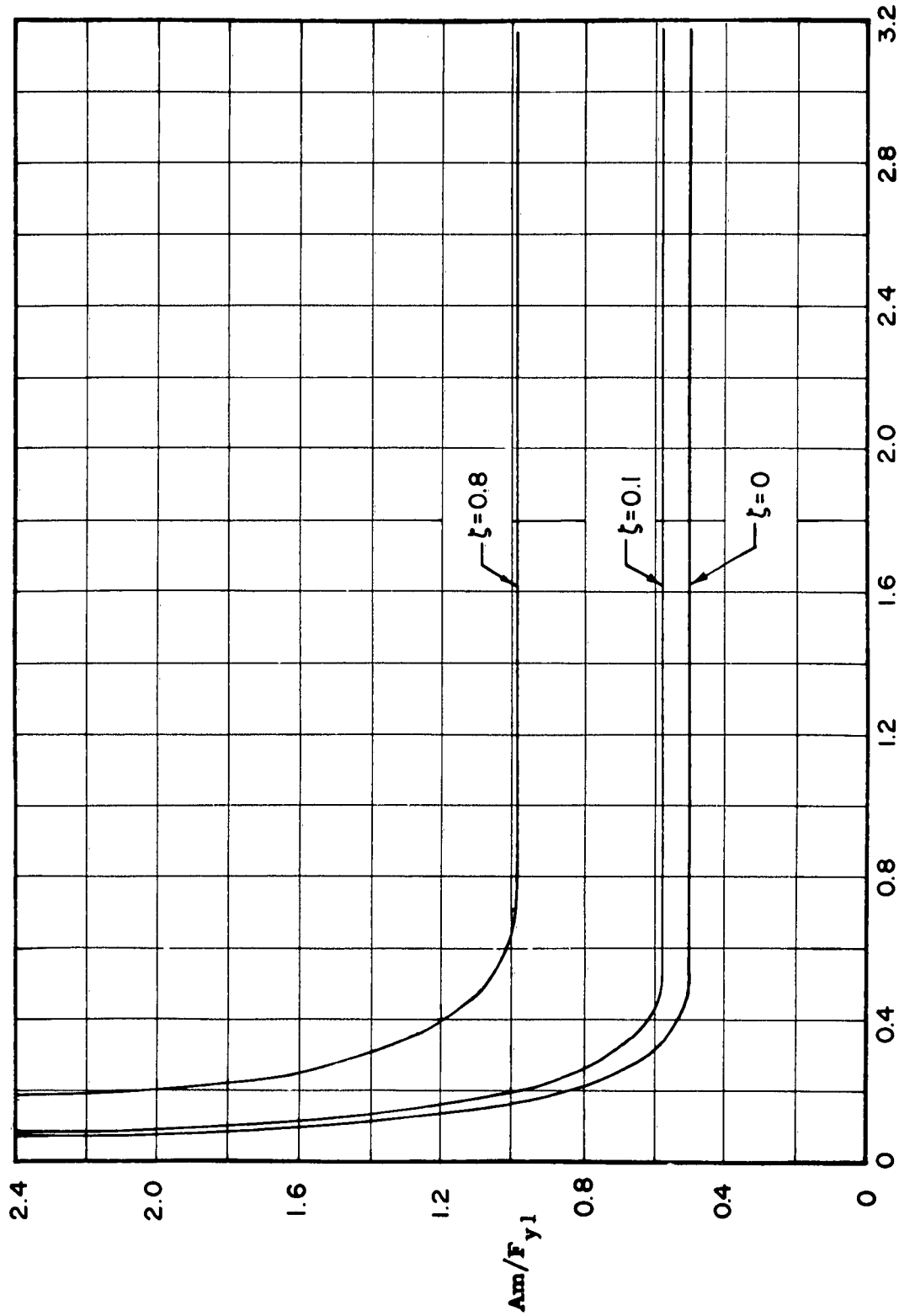

Fig. 17. Rectangular Pulse, Shock Surface, Baselines

the acceleration amplitude to produce permanent deformation that is required when $\zeta = 0$. It may also be noted that if T_d/τ is very small, say less than 0.1, very large acceleration amplitudes are required before permanent deformation can be produced. This minimum value of T_d/τ goes up to about 0.2 when $\zeta = 0.8$. As the pulse duration increases, the permanent deformation appears to become independent of pulse duration. This is an indication of the fact that when maximum deflection is reached before the end of the applied pulse, the deflection becomes independent of the pulse duration. Some of the more important conclusions reached, other than those discussed above, as a consequence of these studies are

1. For a triangular acceleration pulse, with amplitude and rise time fixed, permanent deformation increases as the pulse duration increases indicating that the permanent deformation is also affected by the decay time of the pulse.

2. For small values of T_d/τ, where T_d is decay time, the maximum permanent deformation occurs when t_r/τ is approximately 1/4. For large values of T_d/τ, the maximum permanent deformation occurs at $t_r/\tau = 0$.

3. For a given acceleration pulse, a small amount of damping moves the system to a much lower shock surface and thus produces a significant decrease in permanent deformation. At higher values of the damping factor, the surfaces come closer together.

4. The original design of vehicles which will be air dropped should include as much internal damping as possible to lessen the possibility of damage from aerial delivery.

Multiple-Degree-of-Freedom Systems

To extend the theoretical studies to systems of greater complexity so as to approach somewhat closer an actual vehicle, a study was made of a four-degree-of-freedom system. The particular system considered is shown in Fig. 18. It consists of a cantilever beam made up of three rigid sections pinned end to end, with nonlinear torsional springs holding the sections in alignment. These torsional springs have the moment-angular-displacement relationship shown in Fig. 19. The root of the cantilever is subjected to a prescribed transverse acceleration. By solving four simultaneous second order differential equations, the angular deflections of each segment of the beam can be computed.

The angular displacements produced by a rectangular pulse with an amplitude of 20g and a duration of 60 milliseconds are shown in Fig. 20. Each segment of the model used for these calculations is a beam 5 x 0.25 x 0.25-inch. A moment of 78.1 in.-lb applied at the tip of the model causes each spring to have an angular displacement of 0.04 radians, which is the yield displacement. The moment-displacement curve is the same for each spring. In Fig. 20, the angular displacements θ_A, θ_B, and θ_C represent relative angular displacements between segments as shown in Fig. 18. These angular displacements have been divided by

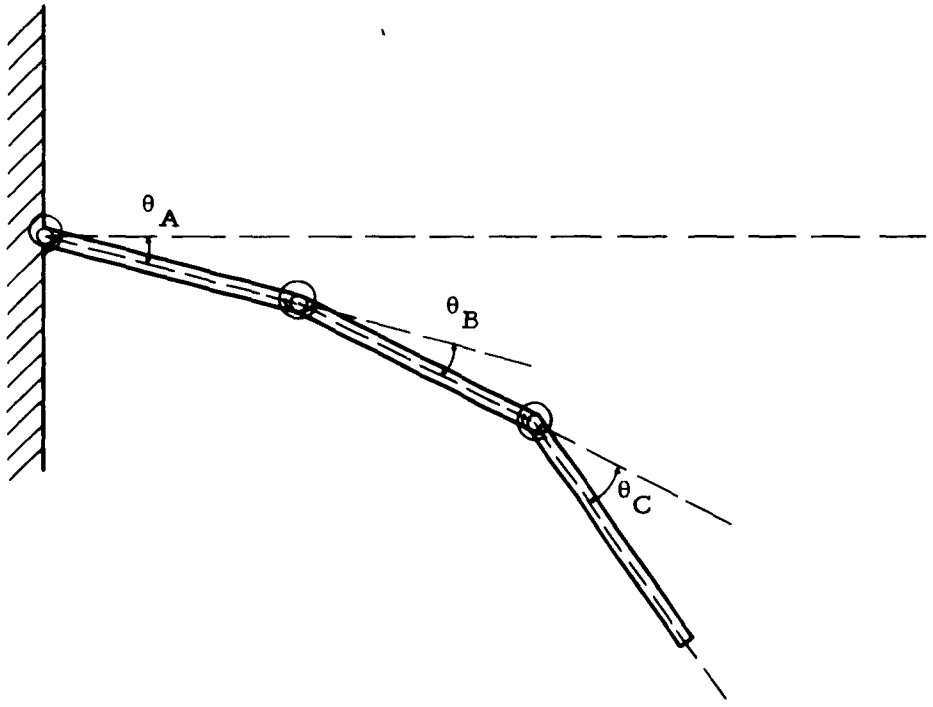

Fig. 18. Positive Angular Displacements

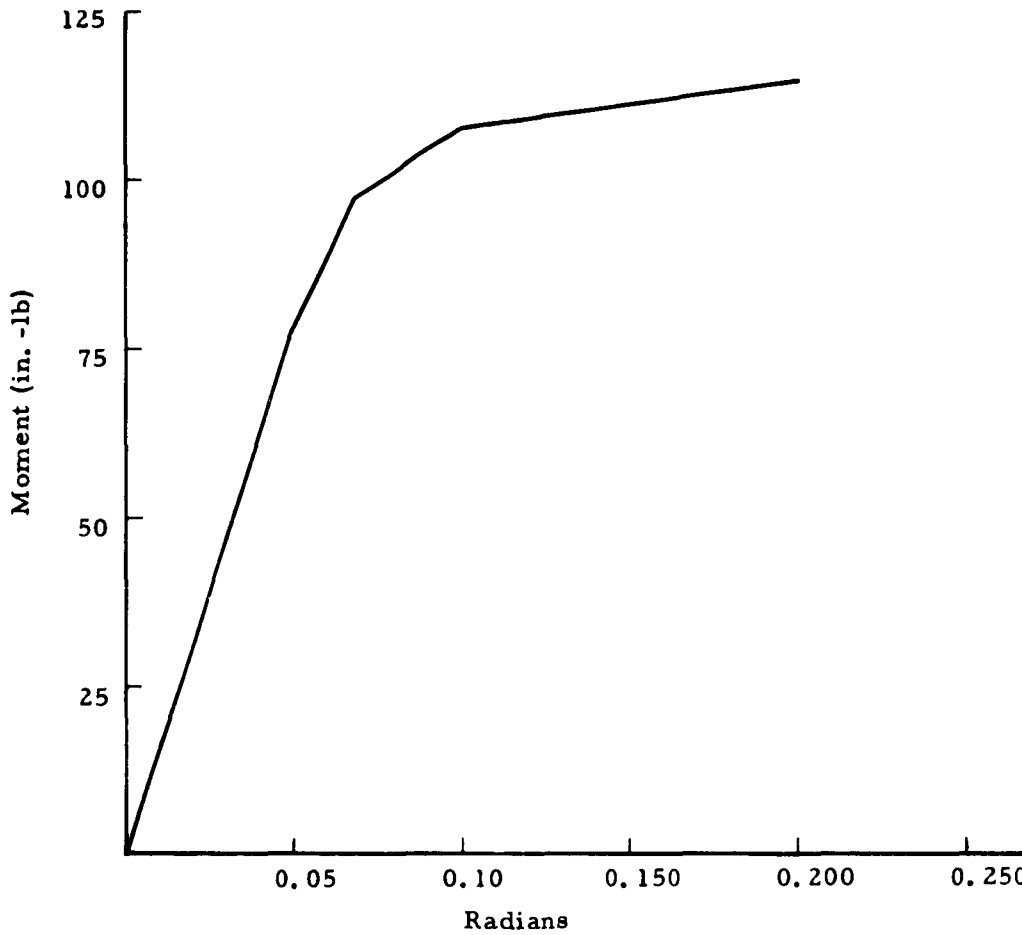

Fig. 19. Moment vs. Angular Displacement for Torsional Spring

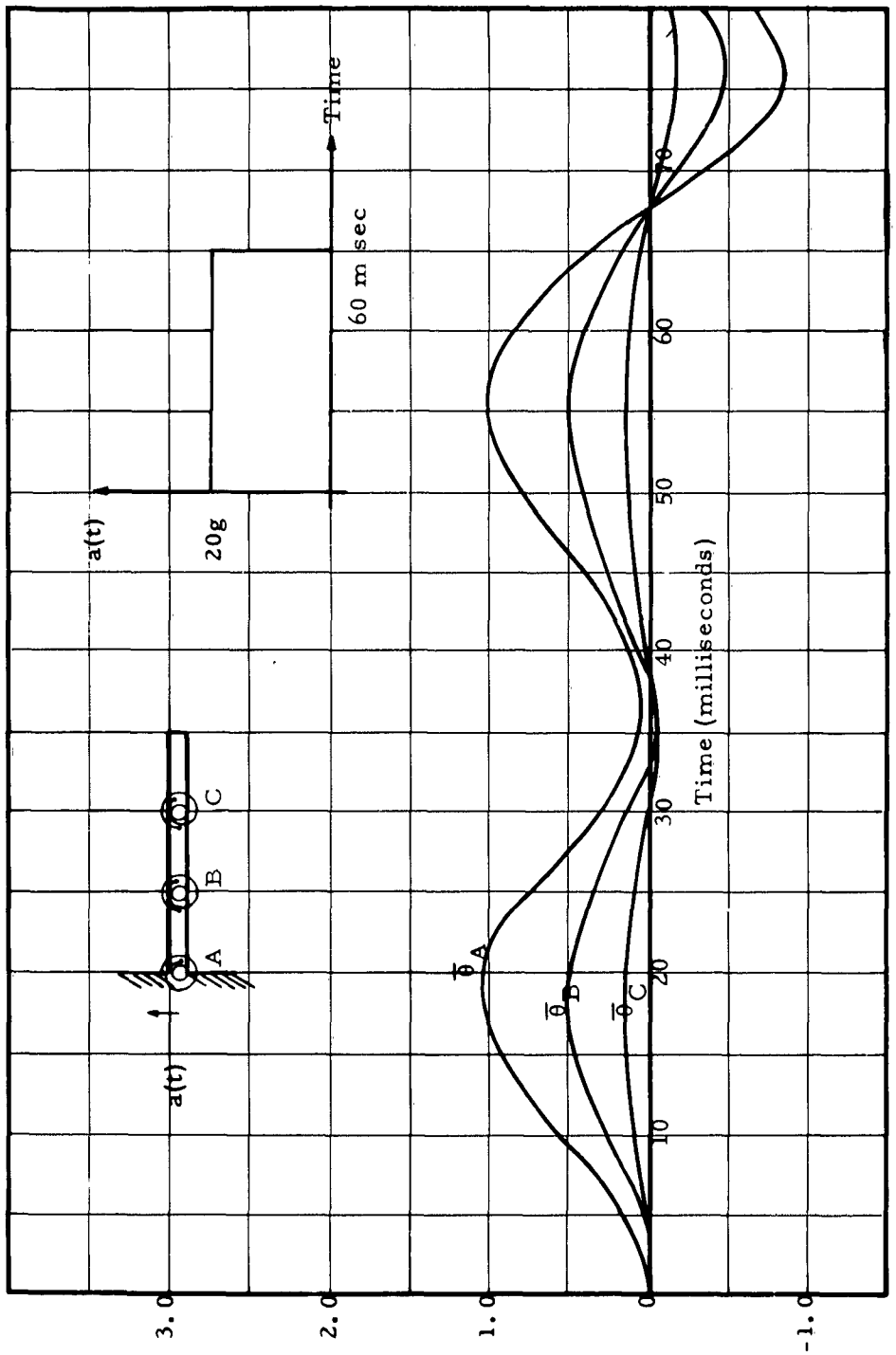

Fig. 20. Nondimensional Angular Displacements vs. Time

the yield displacement to form the ratios $\overline{\theta}_A$, $\overline{\theta}_B$, and $\overline{\theta}_C$ which have been plotted.

Application of the 20g pulse of Fig. 20 produced a permanent angular deformation in the root spring (θ_A) of 0.0038-radians. A similar pulse with an amplitude of 40g produced a permanent angular deformation of 0.070-radians in the root spring. Neither pulse produced permanent deformation in the other two springs. These results indicate that this particular system, when subjected a root acceleration, behaves essentially as a single-degree-of-freedom system. The general shape of the deflection-time curve is determined by the fundamental mode of oscillation, while the minor oscillations superimposed on this curve represent the contributions of the higher modes.

The variation of $\overline{\theta}_{A\ max}$ with the parameter T_d/τ is shown in Fig. 21. This curve is analogous to the one shown in Fig. 16 for the damped single-degree-of-freedom system. The similarity of the curves shown in the two figures provides further substantiation of the statement that the multiple-degree-of-freedom system behaves essentially the same as the single-degree-of-freedom system.

The results of these studies of yielding multiple-degree-of-freedom systems, although not conclusive, when considered with the results of the studies of single-degree-of-freedom systems, indicate that a "fragility" rating might be established by restricting systems to the linear class and considering what combinations of pulse parameters are necessary to push the system up to the boundary represented by

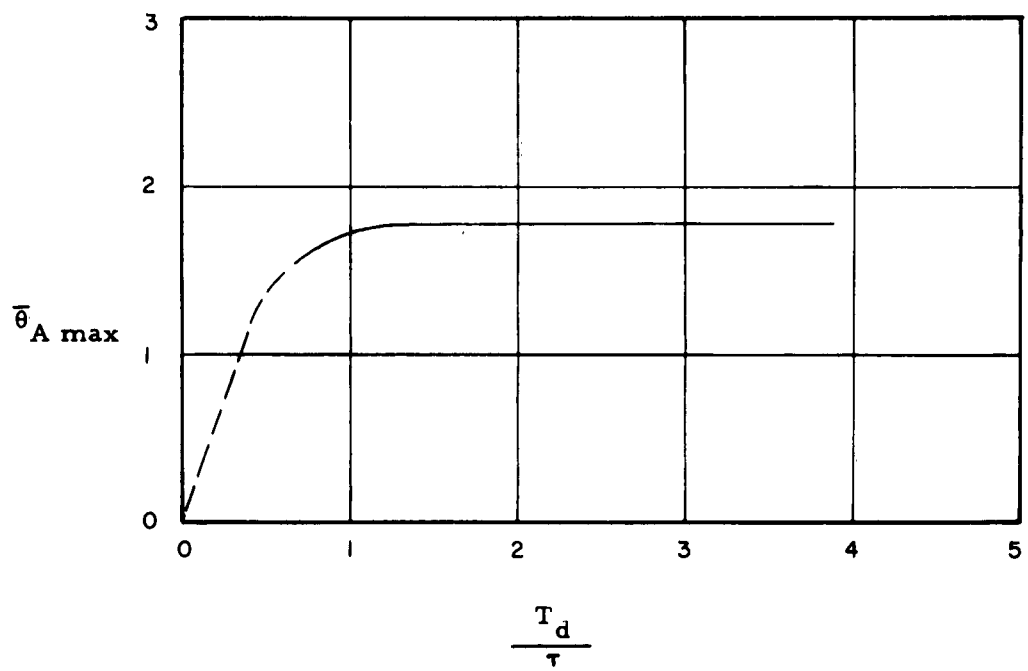

Fig. 21. Cross Section of Shock Spectrum Surface for $A\tau^2/\ell = 1.33$

the shock base line previously discussed. Thus all the information necessary to the design of a cushioning system for a device which can be represented by a simple single-degree-of-freedom system is presented by this single curve, the shock base line.

Cushioning Vehicles with Paper Honeycomb

In order to orient the analytical studies of the cushioning problem more in the direction of actual vehicles and at the same time to retain enough simplicity to make a rational analysis possible, the problem of a cushioned vehicle has been restudied. This study indicates that a reasonably realistic model can be constructed by considering the vehicle to be composed of two masses connected by a spring, and with each mass cushioned with paper honeycomb. This arrangement is illustrated in Fig. 22. In the analysis of the response of this system the important parameter is the relative displacement between the two masses. This displacement is an indicator of the stresses which would be developed as a consequence of the impact. For purposes of the analysis, it is assumed that the entire assembly shown in Fig. 22 is moving at some velocity V_o, when suddenly the platform is brought to rest by an impact. The platform then remains at rest indefinitely. It is also assumed that the cushioning material crushes at a constant stress. No damping is considered. Typical results of this analysis are shown in Fig. 23. The symbols F_1 and F_2 indicate the force exerted by the cushioning material on the two masses, and T is given by the expression

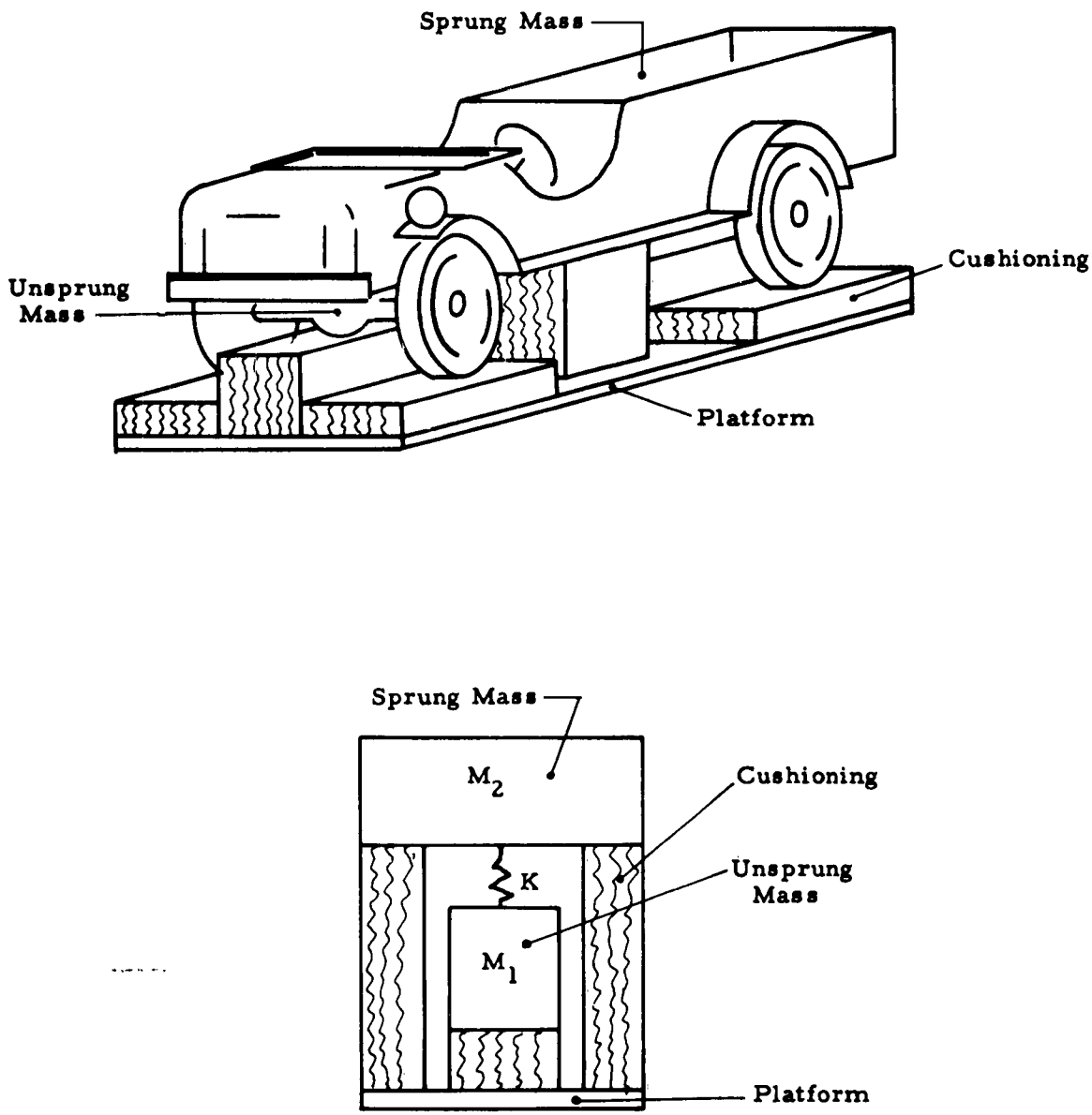

Fig. 22. Simplified Vehicle Model

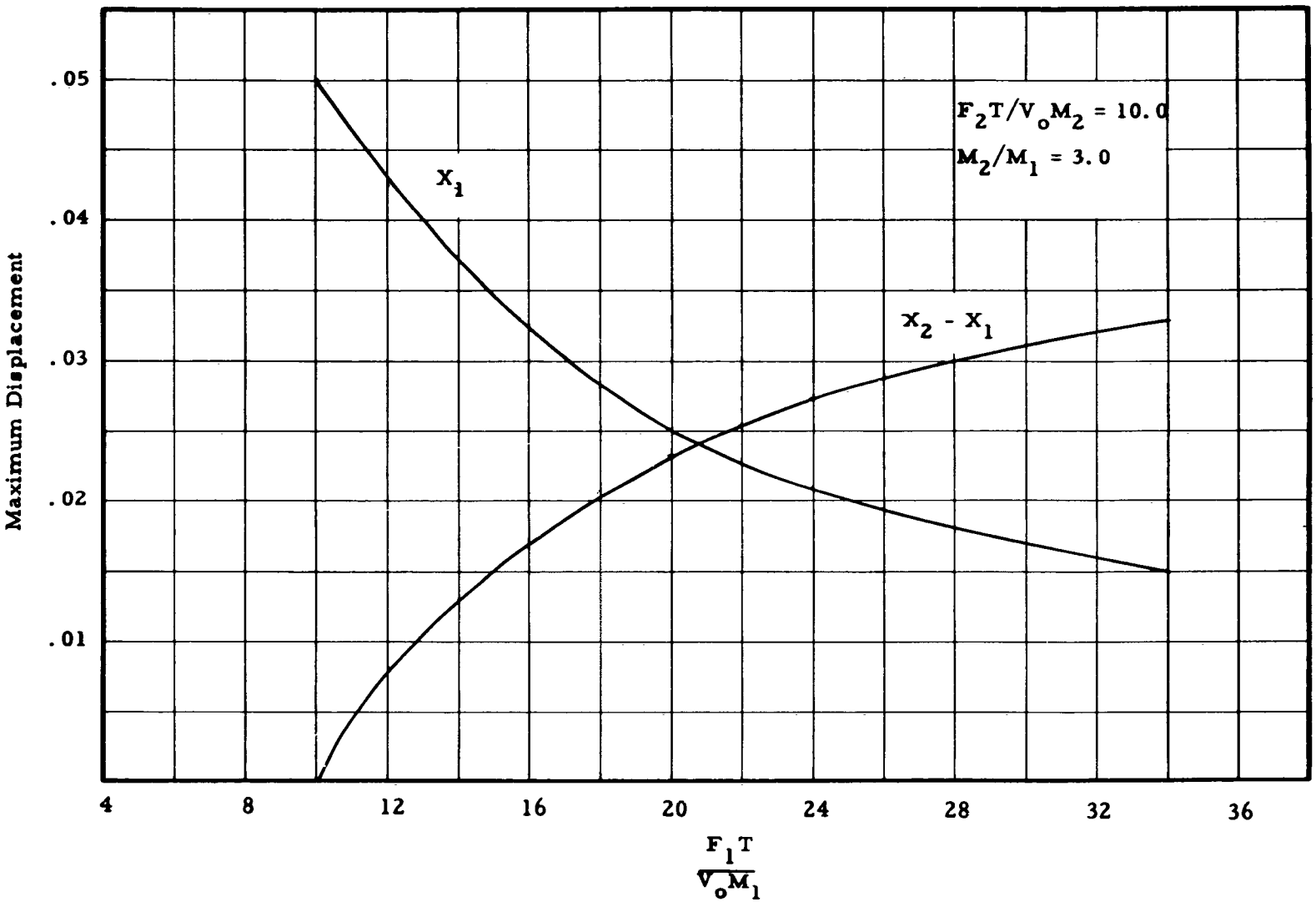

Fig. 23. Maximum Displacements for $M_2/M_1 = 3.0$ and $F_2T/V_oM_2 = 10.0$.

$$T = 2\pi \sqrt{\frac{M_2}{K}}$$

x_1 and x_2 are the nondimensionalized displacements of the two masses. The nondimensionalizing factor is $V_o T$.

Curves such as those in Fig. 23 can be used to design a cushioning system. The procedure is as follows. Specify the maximum allowable values for $(x_2-x_1)_{max}$. Determine the ratio of the two principal masses in the system. Determine T and specify the force F_2. Using the specified value of $(x_2-x_1)_{max}$ pick off the curve the proper value of $F_1 T/V_o M_1$. This specifies the area of cushioning material needed under M_1. Read off the value of x_1 corresponding to the specified value of x_2-x_1. This when divided by the percentage of strain allowed, fixes the minimum thickness for the cushion under M_1. The area of the cushion under M_2 is fixed by the value taken for F_2. This completes the design of the cushioning system. It has been found that this procedure leads to essentially the same design as the procedure heretofore used, based on a maximum acceleration. Thus confidence in the reliability of present cushioning design procedure is substantially increased. Studies, using this approach to the cushioning problem, are continuing and it is expected that a more detailed report of the results will eventually be issued.

PHASE III

Investigation of Resistance to Shock of Specific Vehicles and the Development of Cushioning Systems to Improve the Resistance of these Vehicles to Shock

The objectives of this phase were simply to determine the capacity of selected military vehicles to withstand impacts and to determine the arrangement of cushioning material which would best utilize the capabilities of the equipment. The vehicles used in this investigation were tested essentially in the condition in which they were delivered by the manufacturer, with no local reinforcement, serviced and ready for use. Vehicles which were included in the program are listed as follows.

Utility Truck, 1/4 ton (Jeep)

Cargo Truck M37, 3/4 ton

Cargo Trailer M100, 1/4 ton, 2 wheel

Cargo Trailer M101, 3/4 ton, 2 wheel

Water Tank Trailer XM107E2, 1-1/2 ton

105 mm Howitzer on Carriage M2A2

Cargo Truck M211, 2-1/2 ton

Personnel Carrier M113, Full tracked, armored.

The number of drops per vehicle varied from 4 to 63.

For each drop, accelerations were measured at four or five selected points and high-speed motion pictures were taken. After each drop, the vehicle was carefully inspected for damage and the self-propelled vehicles were road tested.

The significant results obtained for each vehicle are summarized as follows.

Utility Truck, 1/4-Ton

This vehicle was dropped 17 times with design accelerations ranging from 10g to 40g. Drops were made with the vehicle in "as received" condition with the following exceptions

1. Lifting brackets were installed on each wheel hub.
2. The battery box was supported by plywood bracing.
3. The windshield was protected by lashing it between two pieces of honeycomb and strapping it down to the hood.

Data for each of the 17 drops are given in Table I. The recommended cushioning configuration for this vehicle is shown in Fig. 24. This configuration provides a drive-on, drive-off capability.

Typical acceleration records are shown in Fig. 25. Note that the average accelerations and the design accelerations are in substantial agreement. The average acceleration is obtained by dividing the area under the acceleration curve by the time to zero velocity as indicated by the symbol t on the records.

Although the vehicle was damaged somewhat on nearly every drop, it did not become inoperable until after the ninth drop. This difficulty was caused by the starter pedal being bent.

Cargo Truck M37

This vehicle was dropped 8 times with design accelerations ranging

TABLE I. SUMMARY OF DATA FROM DROPS OF 1/4-Ton, 4 x 4 TRUCK

Drop Number	Drop Height	Energy Dissipator	Support System	Design Accel.	Average Accel.	Peak* Accel.	Average Duration of Impact	REMARKS
FR-74	8 ft	80-0-1	2-platform	20 g	13.6 g	24.4g	0.052 sec	No damage
FR-75	14 ft	80-0-1	2-platform	20 g	12.3 g	36.2g	0.077 sec	No damage
FR-76	14 ft	80-0-1/2	2-platform	30 g	18.5 g	49.1g	0.050 sec	Crack in weld and sheet metal between right front fender and body. Slight bending of motor mounts.
FR-77	14 ft	80-0-1/2	2-platform	30 g	20.5 g	64.9g	0.040 sec	Damage to rear frame crossmember and front fender weld. Engine shifted forward approximately 1/8-in.
FR-78	8 ft	80-0-1/2	Honeycomb** WOLS, WSB	20 g	9.9 g	27.3g	0.072 sec	No damage
FR-79	14 ft	80-0-1/2	Honeycomb WOLS, WSB	30 g	19.1 g	42.7g	0.050 sec	Sheet metal buckle in left rear cargo bed at bracket to frame. Slight downward bending of fenders.
FR-80	14 ft	80-0-1/2	Honeycomb WOLS, WSB	30 g	17.2 g	35.2g	0.055 sec	Increase in damage started in FR-79
FR-81	14 ft	80-0-1/2	Honeycomb WOLS, WSB	40 g	25.5 g	50.0g	0.037 sec	Further increase in damage started FR-79; slight bending of engine mounts.
FR-82	14 ft	80-0-1/2	Honeycomb WOLS, WSB	40 g	21.7 g	48.8g	0.043 sec	Increase in body damage. Floorboard and firewall sagging. Right engine mount bent approximately 1 in. Starter pedal bent out of line. Unable to start jeep after drop for first time.
FR-83	8 ft	80-0-1	Honeycomb WLS, WSB	10 g	5.7 g	12.8g	0.120 sec	No damage
FR-84	14 ft	80-0-1/2	Honeycomb WLS, WSB	20 g	10.9 g	26.8g	0.087 sec	Buckle in left rear cargo bed. Floorboard sag.

**See following page

TABLE I. SUMMARY OF DATA FROM DROPS OF 1/4-Ton, 4 x 4 TRUCK (Cont'd)

Drop Number	Drop Height	Energy Dissipator	Support System	Design Accel.	Average Accel.	Peak* Accel.	Average Duration of Impact	REMARKS
FR-85	14 ft	80-0-1/2	Honeycomb WLS, WSB	20 g	NO RECORD- - -			Some floorboard sag and body damage.
FR-86	14 ft	80-0-1/2	Honeycomb WLS, WSB	20 g	11.8 g	31.1g	0.080 sec	Body damage
FR-87	14 ft	80-0-1/2	Honeycomb WLS, WOSB	20 g	15.2 g	30.0g	0.061 sec	Body damage
FR-88	NOT APPLICABLE							
FR-89	NOT APPLICABLE							
FR-90	14 ft	80-0-1/2	Honeycomb WOLS, WOSB	20 g	19.2 g	39.7g	0.049 sec	No damage
FR-91	14 ft	80-0-1/2	Honeycomb WOLS, WOSB	20 g	19.8 g	37.0g	0.048 sec	No damage
FR-92	NOT APPLICABLE							
FR-93	14 ft	80-0-1/2	Honeycomb WOLS, WOSB	20 g	21.4 g	41.0g	0.044 sec	No damage. Approximately 5 fps horizontal velocity

*Highest recorded peak by any of the four accelerometers

**WOLS - without load spreaders
WLS - with load spreaders
WOSB - without spring blocks
WSB - with spring blocks

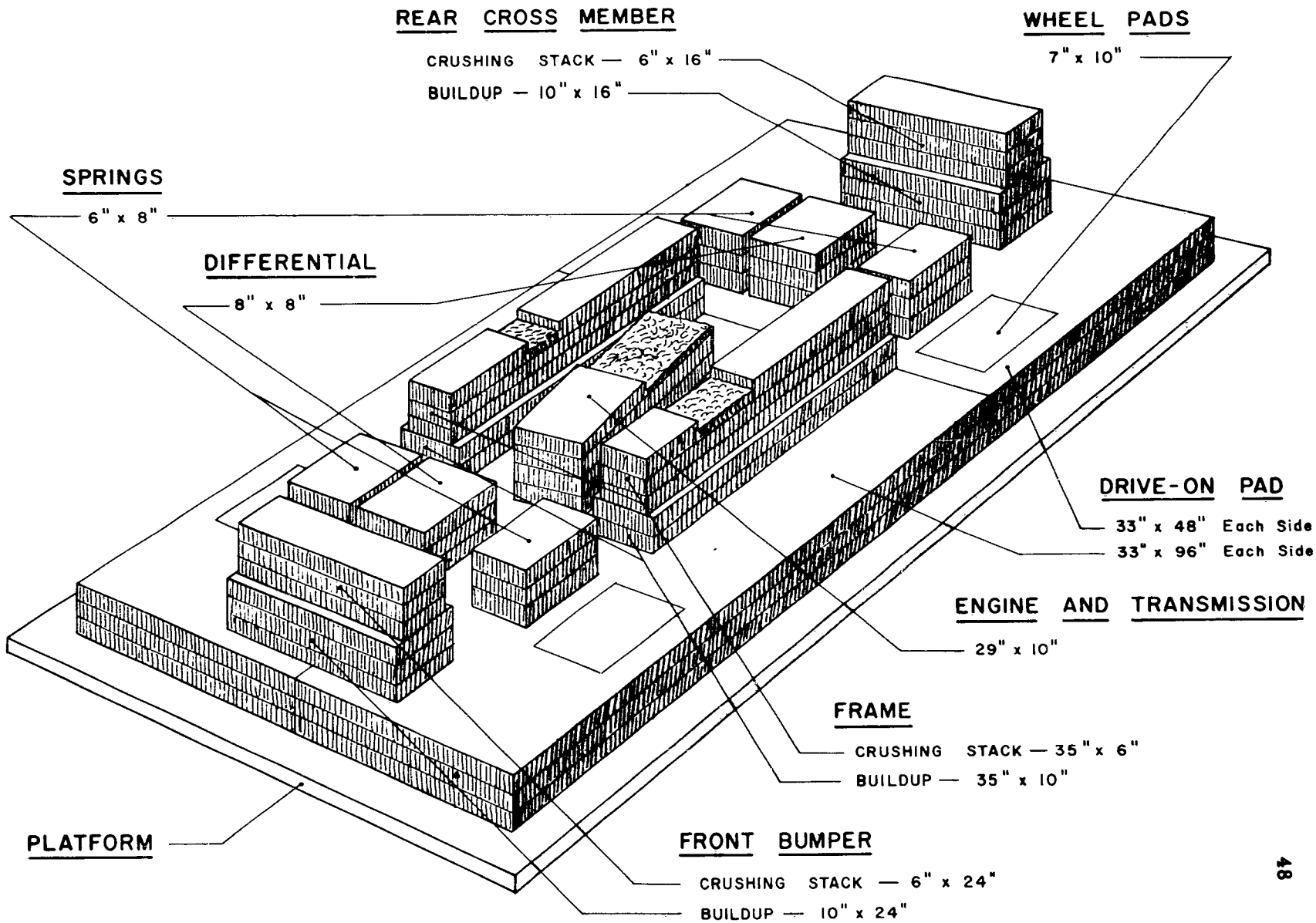

Fig. 24. Recommended Honeycomb Configuration for 1/4-Ton Truck

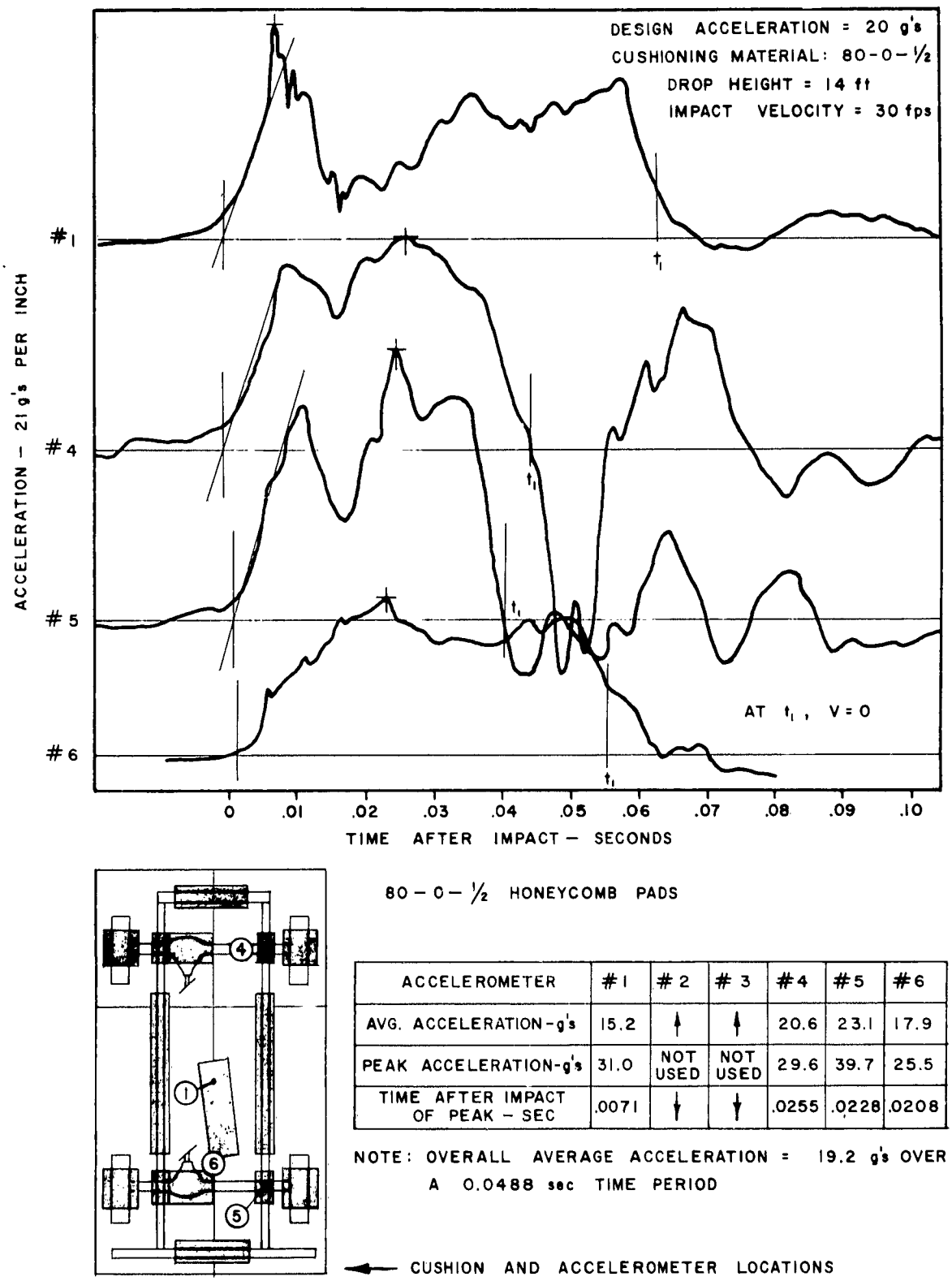

ACCELEROMETER	#1	#2	#3	#4	#5	#6
AVG. ACCELERATION-g's	15.2	↓	↓	20.6	23.1	17.9
PEAK ACCELERATION-g's	31.0	NOT USED	NOT USED	29.6	39.7	25.5
TIME AFTER IMPACT OF PEAK - SEC	.0071	↓	↓	.0255	.0228	.0208

NOTE: OVERALL AVERAGE ACCELERATION = 19.2 g's OVER A 0.0488 sec TIME PERIOD

Fig. 25. A Typical Acceleration Record with Reduced Data for 1/4-Ton Truck

from 10g to 20g. Typical accelerations measured at 5 points on the vehicle are shown in Fig. 26. For the last drop of this vehicle at an impact velocity of 30 fps and with a design acceleration of 16g the measured accelerations were as follows

Location	Average Acceleration, g	Peak Acceleration, g
Left rear axle	17.5	29.0
Right front axle	23.2	33.9
Left frame	8.5	13.5
Right frame	11.3	23.7
Engine	14.5	20.2

The recommended configuration for the cushioning system is shown in Fig. 27. This configuration provides drive-on, drive-off capability.

Damage to the vehicle was restricted to a moderate amount of bending of the center cross members of the frame, and of the oil pan.

Cargo Trailer, 1/4-Ton

This vehicle was dropped 14 times at design accelerations ranging from 14g to 60g. The results of the drops including average accelerations and observed damage are given in Table II. A recommended cushioning configuration is shown in Fig. 27.

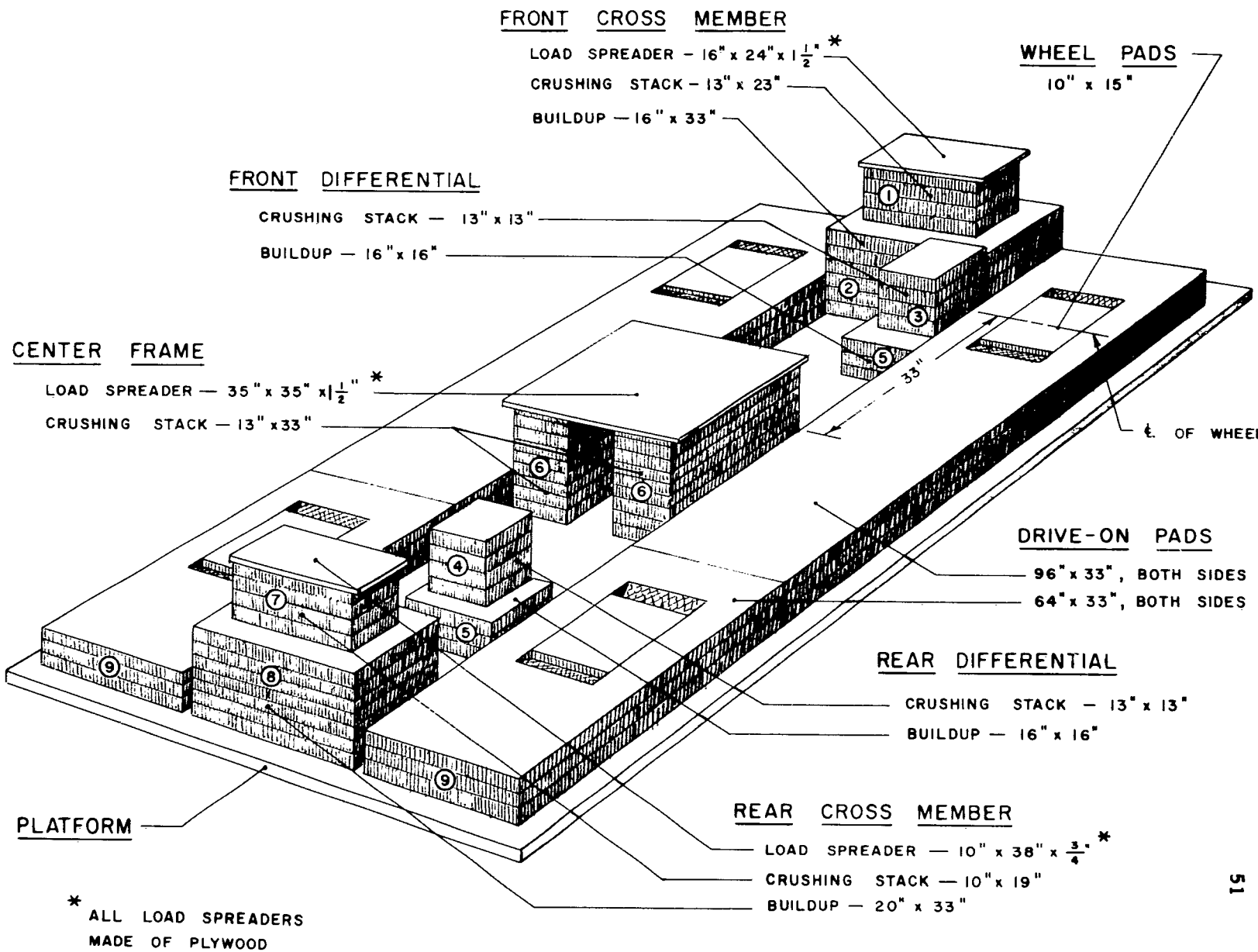

Fig. 26. Recommended Cushioning Configuration for 3/4-Ton Cargo Truck, M37

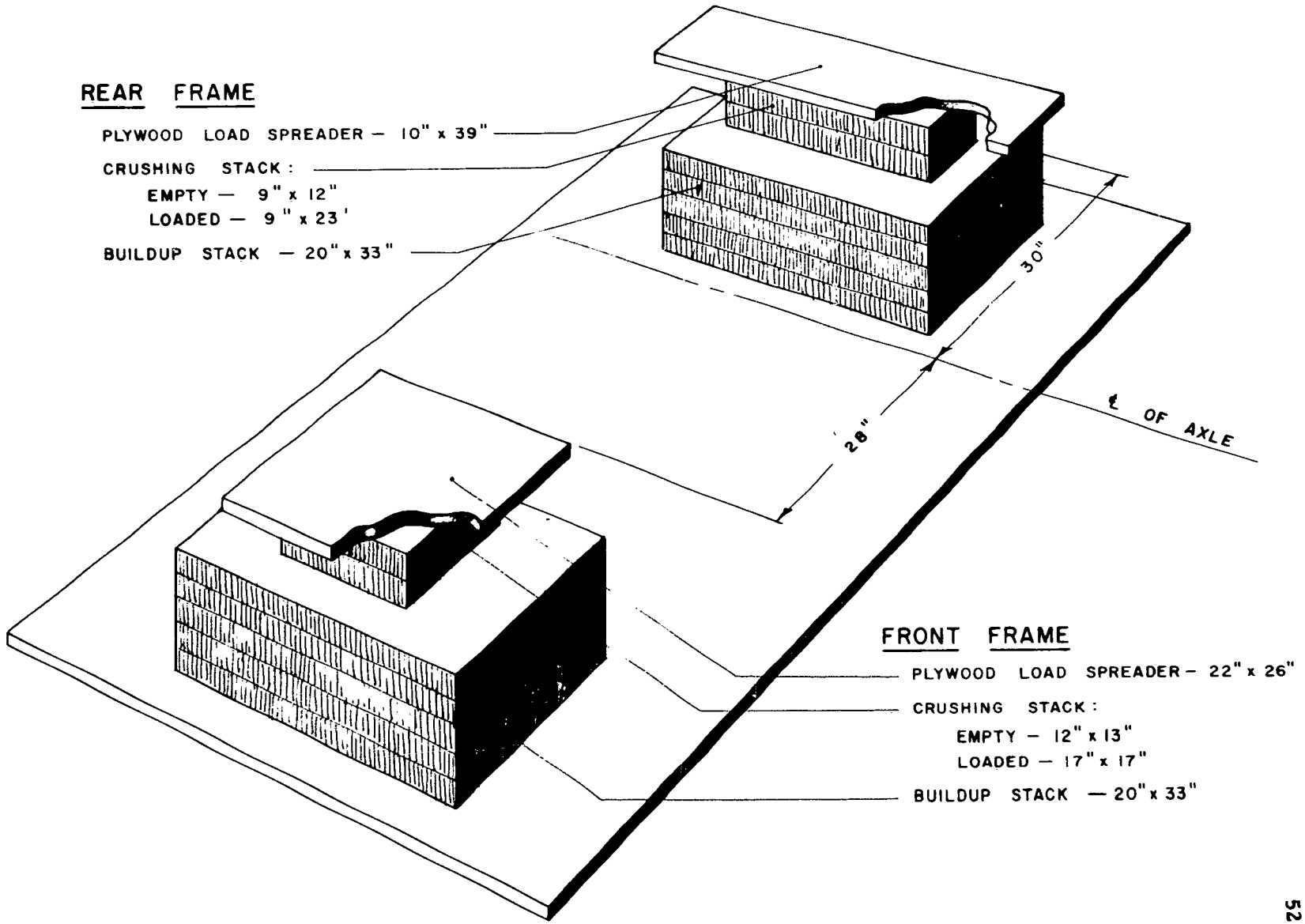

Fig. 27. Recommended Cushioning Configuration for 1/4-Ton Cargo Trailer

TABLE II

SUMMARY OF RESULTS FOR 1/4-TON CARGO TRAILER

Drop No.	Design Accel. (g)	Honey-comb	Frame Avg. (g)	Axle Avg. (g)	Frame Peak (g)	Axle Peak (g)	Average Time of Impact (Sec.)	Average Crushing Under Frame (In.)	Remarks
1	20	80-0-1	12.3	13.9	33.9	24.2	.0742	4.0	No load spreaders. Center of bed bent up about 1/8-inch. Uneven crushing under frame.
2	20	80-0-1	14.1	14.8	47.5	28.2	.0626	5.5	Front load spreader broke and bent brake cables. Uneven crushing under frame.
3	20	80-0-1	12.6	11.4	41.0	26.1	.0682	7.0	More even crushing. No damage.
4	20	80-0-1	17.8	16.8	43.5	26.8	.0532	6.7	Uneven crushing. No damage.
5	20	80-0-1	16.2	15.6	32.5	27.8	.0619	4.7	500-lb load. Front and rear load spreaders broke and bent rear cross members. Uneven crushing.
6	20	80-0-1	16.2	15.3	38.1	22.7	.0583	8.0	Very even crushing. No damage.
7	20	80-0-1	15.4	14.9	35.5	34.2	.0403	7.5	500-lb load. Uneven crushing. Front load spreader broke. No damage to vehicle.
8	14	80-0-1	11.0	11.0	-	25.6	.0852	9.7	500-lb load. Very even crushing. No damage.
9	30	80-0-1/2	19.0	22.9	33.2	42.2	.0463	3.0	Slight bending of bed over rear cross member due to concentrated load.

TABLE II

SUMMARY OF RESULTS FOR 1/4-TON CARGO TRAILER

(Continued)

Drop No.	Design Accel. (g)	Honey-comb	Frame Avg. (g)	Axle Avg. (g)	Frame Peak (g)	Axle Peak (g)	Average Time of Impact (Sec.)	Average Crushing Under Frame (In.)	Remarks
10	50	80-0-1/2	28.2	31.7	69.5	47.6	.0318	2.0	Further bending in bed above rear frame cross member.
11	60	80-0-1/2	34.7	33.5	69.5	57.1	.0272	0.7	Same as Drops 9 and 10.
12	60	80-0-1/2	27.9	31.0	70.8	54.7	.0207	0.5	Changed load spreader design. No apparent damage.
13	30	80-0-1/2	22.3	26.3	56.4	47.2	.0381	2.5	No wheel crushing pads. No damage. Recommended configuration empty.
14	30	80-0-1/2	30.2	32.2	63.3	55.0	.0300	2.7	500-lb load. No wheel crushing pads. Recommended configuration loaded. Front load spreader cracked slightly. No damage to trailer.

Cargo Trailer, 3/4-Ton

This vehicle was studied more extensively than any other vehicle in the program, primarily because it was the first vehicle studied and a need existed at that time for a better insight and feeling for the problem. Also design accelerations were systematically increased to see if a limiting acceleration would be reached at which severe damage would immediately be apparent. A total of 63 drops were made at accelerations ranging from 10g to 90g. Selected results from these drops are shown in Table III. At the beginning of this investigation, it was thought that the maximum acceleration a vehicle could withstand without damage would be the most significant of all parameters which enter into the design of a cushioning system. It gradually became obvious, however, that the cushioning system should be designed to give the minimum acceleration consistent with the properties of the cushioning material available, the desired impact velocity, stability requirements, and mechanical limitations of the arrangement of the cushioning. For most vehicles, the acceleration which might be considered as a limiting value is far above the acceleration which results when the above principles are applied.

The recommended cushioning configuration is shown in Fig. 28.

It should be noted that when one vehicle is dropped repeatedly during a research program, as in the case of the M101 trailer, the damage observed is usually the cumulative effect of all the previous drops. As a consequence, it is not possible to determine definitely

TABLE III

SUMMARY OF RESULTS FOR 3/4-TON CARGO TRAILER

Drop No.	Points of Support	Design Accel. (g)	Impact Velocity (fps)	Energy Dissipator	Frame Avg. (g)	Axle Avg. (g)	Frame Peak (g)	Axle Peak (g)	Average Crushing, Frame (in.)	Remarks
FR-4	3	10	19.6	80-0-1	6.5	6.5	21.6	21.3	6.0*	Frame bottomed on axle. No damage. Unstable.
FR-50	3	20	22.7	80-0-1/2	13.0	11.1	57.8	26.4	3.0*	Wooden blocks between springs and frame. Little rebound.
FR-53	3	30	30.0	80-0-1/2	16.5	13.6	69.3	31.0	8.0*	Rebound about 1 ft. No damage.
FR-55	3	40	30.0	80-0-1/2	17.6	21.4	59.5	36.7	1.2*	Rebound about 2 ft. Tires deflected. Axle bent slightly.
FR-57	3	50	30.0	80-0-1/2	27.8	21.0	84.5	39.2	0.3*	Wheel pads not crushed. Rebound 3 ft. Axle bent.
FR-27	8	Unknown	22.7	QM Shock Pads	16.6	17.5	42.2	36.2	Unknown	Rebound about 1 ft. Axle bent about 1/4-in.

*Average crushing values for the Three-Point Support System are averages of the three crushing stacks.

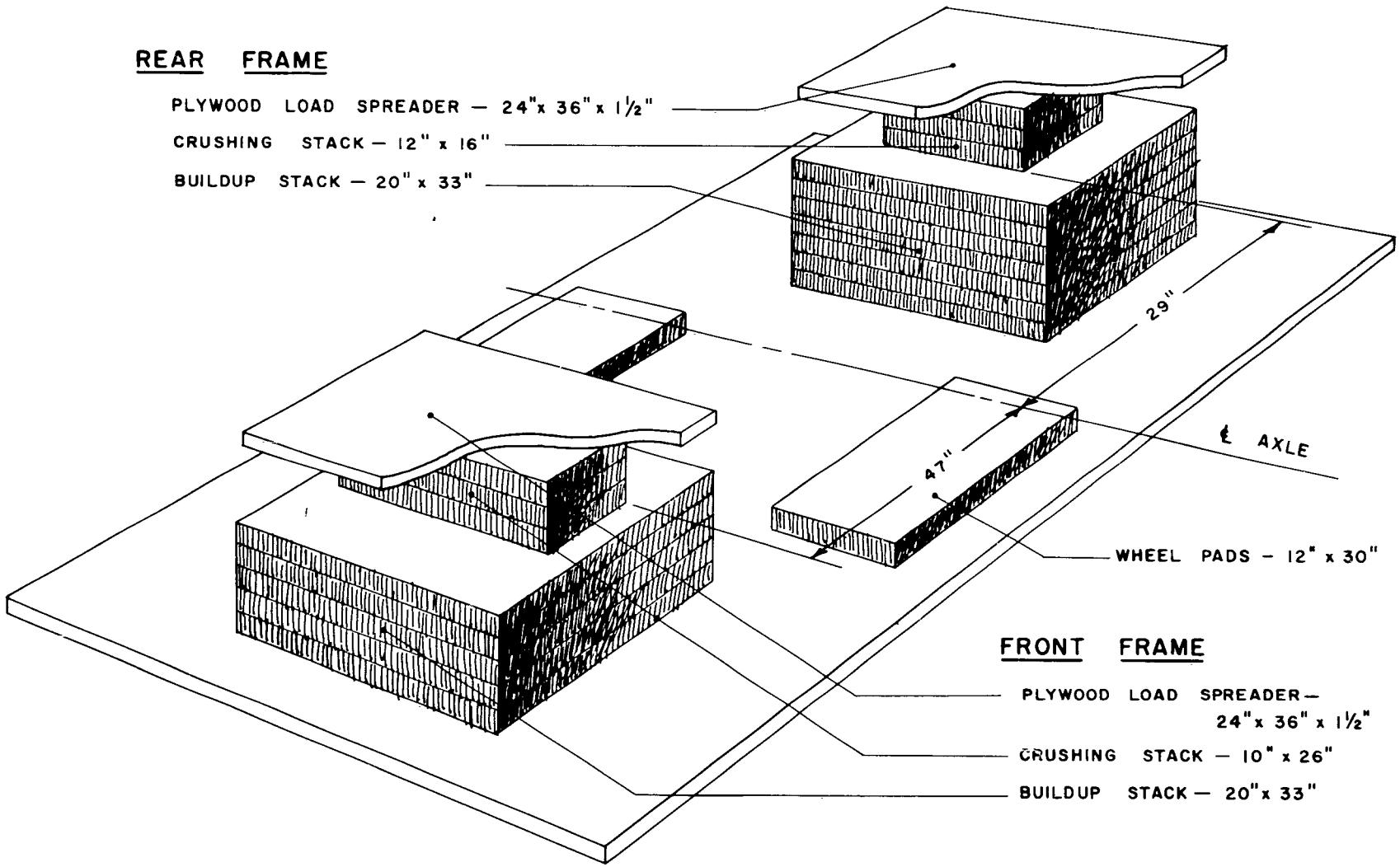

Fig. 28. Recommended Cushioning Configuration for Unloaded 3/4-Ton Trailer Using 80-0-1/2 EDF Paper Honeycomb

which of the many parameters involved is the chief contributor to the damage. If the damage is to be associated successfully with any particular set of parameters it must occur on the first drop.

Water Tank Trailer XM107E2

This vehicle was dropped 23 times at design accelerations ranging from 20g to 100g. The pertinent data for each drop are shown in Table IV. Damage to the vehicle was very limited. Starting with the 50g design acceleration, both fenders began to bend, and after the 100g drop, the outer edge of each fender had deflected permanently about 1/2-inch. After the first 80g drop, the axle was observed to be bent about 1/4-in. out of line at the mid-point.

In 2 of the drops, made at 30g, a horizontal component of velocity of about 3 fps was given to the trailer. This produced some slip between honeycomb pads which were not glued, but the over-all effect was insignificant.

A recommended configuration of the cushioning system for this vehicle is shown in Fig. 29.

105 mm Howitzer

A total of 7 drops was made at design accelerations ranging from 10g to 40g and impact velocities from 25 fps to 30 fps. No damage was sustained even though a peak acceleration of 61g was measured on the barrel in the 40g drop. Representatives of a nearby National Guard unit checked the howitzer after this series of drops and reported satisfactory operation.

TABLE IV

SUMMARY OF RESULTS FOR WATER-TANK TRAILER

Drop No.	Points of Support	Design Accel. (g)	Impact Velocity (fps)	Energy Dissipator	Average Frame Accel. (g)	Average Axle Accel. (g)	Peak Frame Accel. (g)	Peak Axle Accel. (g)	Average Duration of Frame Impact	Average Crushing, Frame (in.)
FR-58	6	20	22.5	80-0-1	9.2	9.5	28.6	19.9	.078	2.5
FR-59	6	40	30.0	80-0-1/2		INSTRUMENTATION				1.8
FR-60	6	40	30.0	80-0-1/2		MALFUNCTION				2.0
FR-61	6	40	30.0	80-0-1/2		NO ACCELERATION DATA				2.3
FR-62	6	40	30.0	80-0-1/2	17.3	21.4	35.6	43.8	.053	1.8
FR-63	6	50	30.0	80-0-1/2	19.3	20.7	62.3	48.1	.047	2.1*
FR-64	6	50	30.0	80-0-1/2	23.4	25.8	47.4	48.7	.039	1.0
FR-65	6	50	30.0	80-0-1/2	17.2	20.5	63.4	39.4	.051	2.5*
FR-66	6	60	30.0	80-0-1/2	25.5	25.3	118.2	53.9	.038	1.0
FR-67	6	60	30.0	80-0-1/2	23.9	25.3	87.4	50.8	.041	1.0
FR-68	6	70	30.0	80-0-1/2	20.5	28.0	79.6	65.6	.046	1.3*
FR-69	6	70	30.0	80-0-1/2	24.0	28.6	89.9	55.7	.041	1.0

*Pads serrated.

TABLE IV. SUMMARY OF RESULTS FOR WATER-TANK TRAILER

(Cont'd)

Drop No.	Points of Support	Design Accel. (g)	Impact Velocity (fps)	Energy Dissipator	Average Frame Accel. (g)	Average Axle Accel. (g)	Peak Frame Accel. (g)	Peak Axle Accel. (g)	Average Duration of Frame Impact	Average Crushing, Frame (in.)
FR-70	6	80	30.0	80-0-1/2	25.4	27.4	102.0	39.5	.037	1.3*
FR-71	6	80	30.0	80-0-1/2	30.6	30.7	101.0	55.7	.032	0.7
FR-72	6	100	30.0	80-0-1/2	33.9	28.4	111.8	62.8	.028	0.4
FR-73	6	100	30.0	80-0-1/2	34.5	26.5	117.1	59.4	.028	0.6*
FR-88	6	30	30.0	80-0-1	14.8	19.1	26.0	28.6	.059	3.8
FR-89	6	30	30.0	80-0-1/2	11.7	16.6	21.1	28.0	.063	4.4
FR-124	4	20	30.0	80-0-1	18.5	14.7	25.3	21.8	.067	3.9
FR-125	4	20	30.0	80-0-1/2	-	15.4	-	26.1	Load Spreaders Broke	
FR-126	4	15	30.0	80-0-1	10.8	9.5	21.8	18.8	.085	7.0
FR-137	5	18	30.0	80-0-1/2	18.3	18.7	31.6	31.0	.051	9.0
FR-138	5	20	30.0	80-0-1/2	17.9	22.6	34.7	46.6	.052	7.5

*Pads serrated.

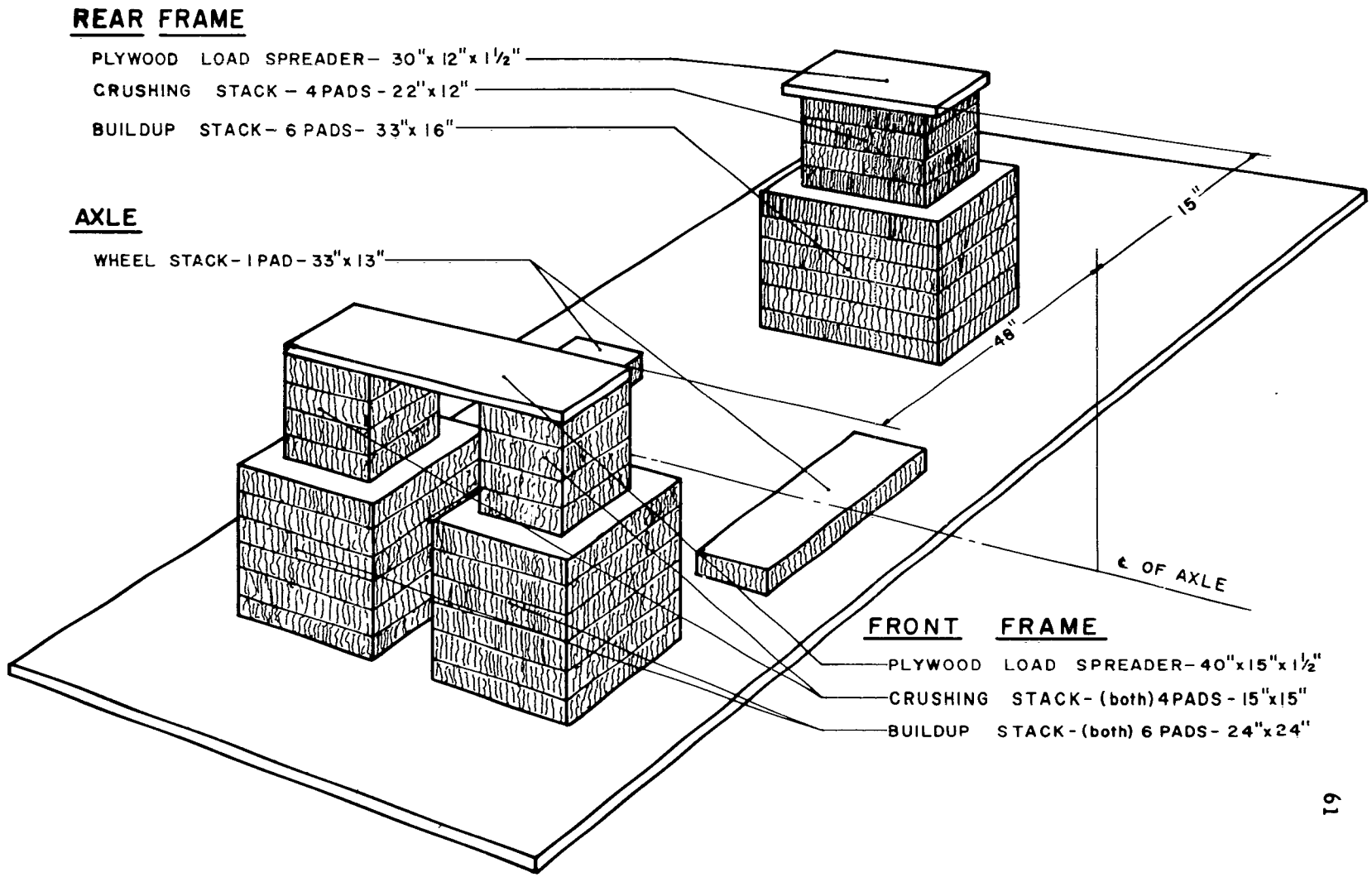

Fig. 29. Recommended Cushioning Configuration for Water-Tank Trailer

The test program on the howitzer was discontinued before it was completed to devote attention to other more urgent aspects of the vehicle program.

Cargo Truck M211, 2-1/2-Ton

This vehicle was dropped 4 times with a design acceleration of 20g and an impact velocity of 25 fps. An effort was made to keep the number of stacks of honeycomb to a minimum. As a consequence, for the first drop, honeycomb was placed under the wheels, differentials, engine, and transmission with load spreaders on the wheel pads. This arrangement proved to be inadequate and the engine-mount bolts sheared, and the frame bent slightly. For the second drop, the wheel-pad area was reduced and the engine and transmission pads were increased in area. After the drop, a further increase in frame bending and some bending of the rear axle was noted. For the next two drops, a load spreader was used under the main frame and the honeycomb area under the wheels was reduced. No further damage occurred.

The pad sizes used for the final cushioning configuration are as follows

1.	Front bumper	20 x 26 x 9 in.
2.	Differentials	22 x 22 x 9 in.
3.	Front wheels	12 x 12 x 9 in.
4.	Frame	9 x 92 x 9 in.
5.	Frame	10 x 60 x 9 in.
6.	Rear wheels	12 x 24 x 9 in.
7.	Rear bumper	15 x 33 x 9 in.

These are the pad sizes required for cushioning. Additional honeycomb is required in general to bring these pads to the height of the member they support.

Personnel Carrier M113

This was the only tracked vehicle included in the program. It was dropped a total of 8 times, 7 times at 25 fps, and once at 16 fps. The air-drop weight of this vehicle is 18, 500 lb, with 15, 375 lb in the hull, and 3, 125 lb in the track assembly. Due to the broad, flat under surface of the hull of this vehicle, the cushioning configuration recommended for it is quite simple. The configuration is shown in Fig. 30. In this configuration, a drive-on pad is shown which provides the only cushioning under the tracks. It is possible to safely drop this vehicle without any cushioning whatsoever under the tracks. This was done twice in the test series. Peak accelerations as high as 280g were measured on the road wheels during these drops with an average as high as 222g. The vehicle was inspected for damage after each drop, and then was driven to check for damage not apparent in a visual inspection. At the end of the eighth drop, the vehicle was still operating, but some damage was evident. For example, the periscope mounting brackets began to bend after the fifth drop. After the sixth drop, one bolt in the driver's instrument panel pulled out, and a knocking sound could be heard from the rear of the engine. After the seventh drop, which was the first without cushioning under the tracks, the hydraulic system

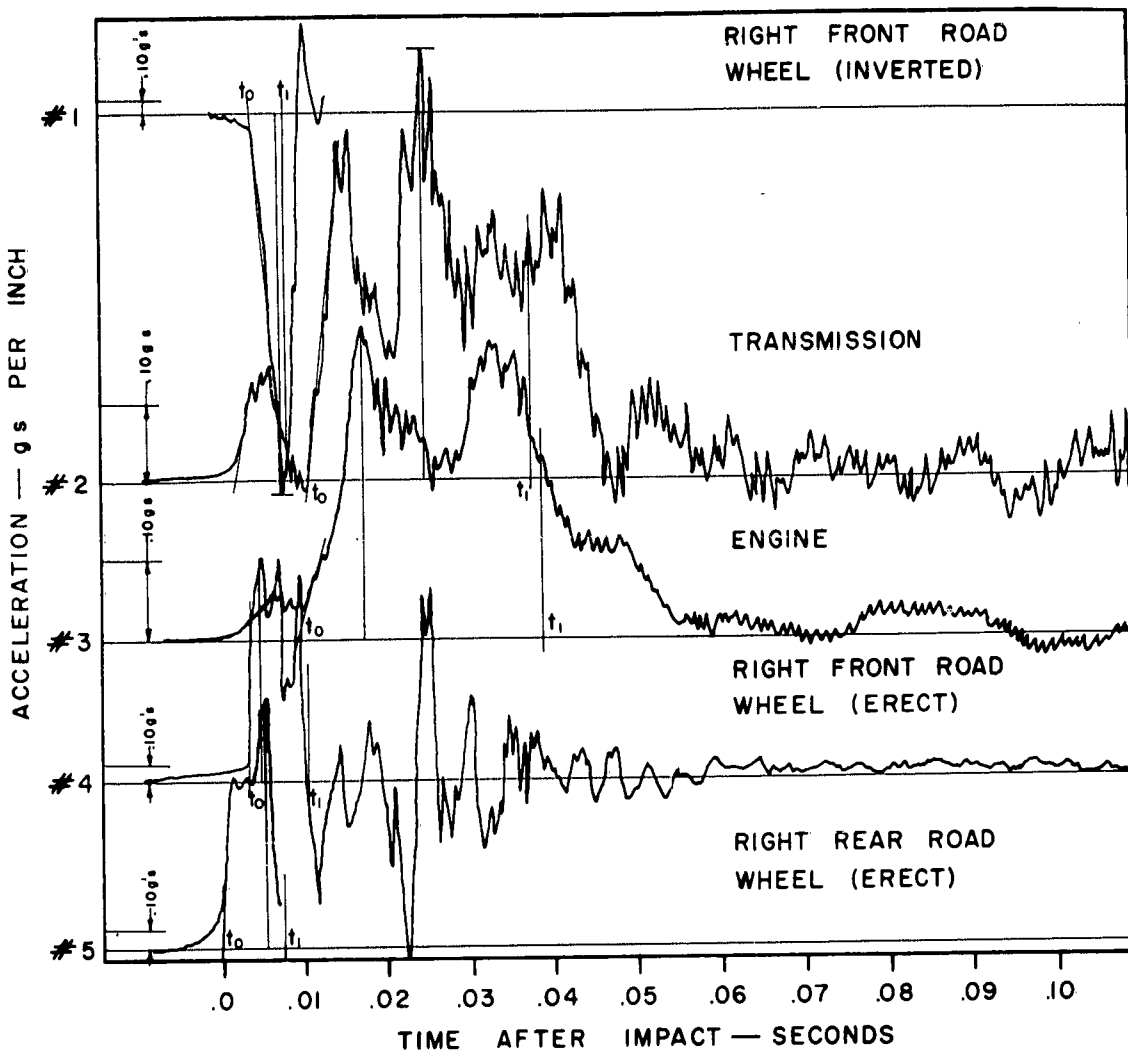

ACCELEROMETER	#1	#2	#3	#4	#5	#6
AVG. ACCELERATION	222	29.6	27.1	NOT USED	109	112
PEAK ACCELERATION	280	55.8	41.5		188	194
TIME OF PEAK	.00239	.0137	.00399		.00159	.00478

Note: Accelerations Are Expressed In Dimensionless g's

Fig. 30. Accelerometer Record for Drop FR-147 of the M113 Personnel Carrier, Impact Velocity 25 fps

for raising and lowering the ramp on the rear of the vehicle was inoperative. This probably represented cumulative damage. After the final drop, which was the second without cushioning under the tracks, a small crack was observed in the left rear mount of the transfer case. The cushioning configuration used for this last drop probably is on the borderline of what is necessary for adequate protection; but it seems very likely that if this configuration had been used for the first drop, no visible damage would have occurred. Where clearances in delivery aircraft are extremely small and drops are to be made on soil instead of concrete, the cushioning under the tracks could very well be omitted.

PHASE IV

Design of Cushioning Systems for Air Delivery of Equipment

The objective in this phase was to prepare what might be termed a handbook for the designer of cushioning systems. In the compilation which was prepared and given the title shown above, the air-delivery process is discussed. This is followed by a consideration of stress-strain, energy-dissipation characteristics of materials in which the terms used in cushioning design are defined and the basic ideas regarding energy dissipation with crushable materials are introduced. The theory of cushioning with crushable materials is discussed using the maximum acceleration to which the vehicle or device is to be subjected as the principal design criterion. Properties of various cushioning materials are discussed and stress-strain curves for paper honeycomb, foamed plastics, aluminum honeycomb, and other materials and systems are presented. A cushioning system for a hypothetical vehicle is designed, and then cushioning systems for two vehicles which were included in the Phase III program are discussed.

The material presented in this compilation is representative of the state of the art at the time of publication, August 1961. This is a rapidly developing field. Consequently, much of the information now in the "handbook" will eventually become obsolete. New editions will have to be issued from time to time if the "handbook" is to be kept up to date.

CONCLUSION

Obviously it has been necessary to omit many of the details of each research program in this brief summary. Readers who are interested in obtaining more complete information can locate the original source from which the information contained in this final report was compiled by consulting the bibliography which follows. All reports which have been issued under Contract DA-19-129 QM 1383 are listed in the bibliography.

BIBLIOGRAPHY

1. Memorandum Report
   Additional Test Data on Foamed Plastics 108C
   August 4, 1959

2. Memorandum Report
   Additional Test Data on Foamed Plastics 100C
   August 5, 1959

3. Turnbow, J. W. and Wm. Ogletree, Energy-Dissipating Characteristics of Airbags, August 1959

4. Memorandum Report
   3/4-Ton Cargo Trailer and 1-1/2-Ton Two-Wheel Water Tank Trailer, B. C. Ellis, September 1959

5. Letter Report
   2-1/2-Ton Cargo Truck, Albert Richter
   September 1959

6. Memorandum Report
   M-37, 4 x 4 Cargo Truck, 3/4-Ton
   December 1959

7. Memorandum Report
   M-37, 4 x 4 Cargo Truck, 3/4-Ton
   January 26, 1960

8. Memorandum Report
   1/4-Ton, 4 x 4 Utility Truck
   January 1960

9. Memorandum Report
   Tests Performed on the Latest Shipment of Type 100C Foamed Plastics
   January 1960

10. Covington, Clarke, Robert Luke, Albert Richter, and Richard Shield, Fragility Studies, Part I, Utility Truck, 1/4-Ton
    March 7, 1960

11. Memorandum Report
    M100, 1/4-Ton, 2-Wheel Cargo Trailer
    April 1, 1960

12. Covington, Clarke, and Richard Shield, Fragility Studies, Part II, Cargo Truck, M37, 3/4-Ton, April 12, 1960

13. Covington, Clarke, and Richard Shield, Fragility Studies, Part III, Cargo Trailer, M100, 1/4-Ton, 2-Wheel, May 3, 1960

14. Luke, Robert R., The Impact Response of a Single-Degree-of-Freedom System with Viscous Damping, June 16, 1960

15. Richter, Albert P., Jr., The Response of a Two-Degree-of-Freedom Undamped System Subjected to Impulsive Loading, August 1960

16. Shield, Richard, and Clarke Covington, Fragility Studies, Part IV, Cargo Trailer, M101, 3/4-Ton, August 1960

17. Shield, Richard, and Clarke Covington, Fragility Studies, Part V, Water Tank Trailer, XM107E2, 1-1/2-Ton, September 1960

18. Shield, Richard, and Clarke Covington, High-Velocity Impact Cushioning, Part VI, 108C and 100C Foamed Plastics, September 1960

19. Huckabay, James D., A Study of the Plastic Deformation of a Single-Degree-of-Freedom System Subjected to Impulsive Loading, January 1961

20. Research Memorandum
Impact Tests of a Rigid Polyurethane Foam, QM 1-61
March 21, 1961

21. Energy-Dissipation Characteristics, Freeman Chemical Company-Foamed Plastics, SMRL-QM 2-61
May 1961

22. Ellis, Billy C., E. A. Ripperger and J. Neils Thompson, Design of Cushioning Systems for Air Delivery of Equipment, August 1961

23. Fowler, Wallace, An Analytical Study of an Undamped Nonlinear Single-Degree-of-Freedom System Subjected to Impulsive Loading, January 1962

24. Reifel, Michael D., The Effects of Acceleration Pulse Parameters on the Permanent Deformation of a Damped Single-Degree-of-Freedom System, January 1962

25. Fowler, Wallace, High-Velocity Impact Cushioning, Part VI, Personnel Carrier, M113, July 1962

26. Ford, Charles A., Further Studies of the Response to Shock Loading of Vehicles Cushioned for Aerial Delivery, October 1962
This report will be issued under Contract DA 19-129 AMC2096(X) (OI 7003)

AD_____Accession No._____

Structural Mechanics Research Laboratory
The University of Texas, Austin, Texas

Impact Determinations
E. A. Ripperger

Final Report, October 26, 1962, 80 pp
figures and tables
(Contract DA 19-129-QM-1383) O. I. No. 9118
Unclassified Report

All of the investigations completed under Contract DA 19-129-QM-1383 are summarized. This includes studies of cushioning materials, analyses of mathematical models which are pertinent to the problem of aerial delivery, studies of the reactions of specific vehicles to impact loading, and the cushioning "handbook" in which the state of the art of cushioning for aerial delivery is presented. A bibliography of all reports issued under this contract is included.

Unclassified

1. Final Report - Impact Determinations
2. Contract DA 19-129-QM-1383

AD_____Accession No._____

Structural Mechanics Research Laboratory
The University of Texas, Austin, Texas

Impact Determinations
E. A. Ripperger

Final Report, October 26, 1962, 80 pp
figures and tables
(Contract DA 19-129-QM-1383) O. I. No. 9118
Unclassified Report

All of the investigations completed under Contract DA 19-129-QM-1383 are summarized. This includes studies of cushioning materials, analyses of mathematical models which are pertinent to the problem of aerial delivery, studies of the reactions of specific vehicles to impact loading, and the cushioning "handbook" in which the state of the art of cushioning for aerial delivery is presented. A bibliography of all reports issued under this contract is included.

Unclassified

1. Final Report - Impact Determinations
2. Contract DA 19-129-QM-1383

AD_____Accession No._____

Structural Mechanics Research Laboratory
The University of Texas, Austin, Texas

Impact Determinations
E. A. Ripperger

Final Report, October 26, 1962, 80 pp
figures and tables
(Contract DA 19-129-QM-1383) O. I. No. 9118
Unclassified Report

All of the investigations completed under Contract DA 19-129-QM-1383 are summarized. This includes studies of cushioning materials, analyses of mathematical models which are pertinent to the problem of aerial delivery, studies of the reactions of specific vehicles to impact loading, and the cushioning "handbook" in which the state of the art of cushioning for aerial delivery is presented. A bibliography of all reports issued under this contract is included.

Unclassified

1. Final Report - Impact Determinations
2. Contract DA 19-129-QM-1383

AD_____Accession No._____

Structural Mechanics Research Laboratory
The University of Texas, Austin, Texas

Impact Determinations
E. A. Ripperger

Final Report, October 26, 1962, 80 pp
figures and tables
(Contract DA 19-129-QM-1383) O. I. No. 9118
Unclassified Report

All of the investigations completed under Contract DA 19-129-QM-1383 are summarized. This includes studies of cushioning materials, analyses of mathematical models which are pertinent to the problem of aerial delivery, studies of the reactions of specific vehicles to impact loading, and the cushioning "handbook" in which the state of the art of cushioning for aerial delivery is presented. A bibliography of all reports issued under this contract is included.

Unclassified

1. Final Report - Impact Determinations
2. Contract DA 19-129-QM-1383